THE UNIVERSITY OF CALGARY

BER Reduction Techniques Of DSSS Over Flat Fast Fading Channels

by

Adikarige Shavantha Arunjith Kularatna

A THESIS

SUBMITTED TO THE FACULTY OF GRADUATE STUDIES

IN PARTIAL FULFILLMENT OF THE REQUIREMENTS FOR THE

DEGREE OF MASTER OF SCIENCE

DEPARTMENT OF ELECTRICAL AND

COMPUTER ENGINEERING

CALGARY, ALBERTA

SEPTEMBER, 1995

THE UNIVERSITY OF CALGARY

FACULTY OF GRADUATE STUDIES

The undersigned certify that they have read, and recommend to the Faculty of Graduate Studies for acceptance, a thesis entitled, "BER REDUCTION TECHNIQUES OF DSSS OVER FLAT FAST FADING CHANNELS", submitted by Adikarige Shavantha Arunjith Kularatna in partial fulfillment of the requirements for the degree of Master of Science.

Michel Fattouche

Supervisor, ~~Dr. Michel~~ Fattouche
Dept. of Elec. and Comp. Engg.

B.R. Petersen

Dr. Brent Petersen
Dept. of Elec. and Comp. Engg.

Dr. S. T. Nichols
Dept. of Elec. and Comp. Engg.

H. Zaghloul

Dr. Hatim Zaghloul
President and C.E.O. Wi-LAN Inc.

Date: Sept. 26, 95

ABSTRACT

Irreducible bit error rate is created when a narrowband (25kHz) DSSS signal is transmitted over a flat fast fading channel in an urban environment such as in wide area paging. Phase distortion due to fast fading is the main cause of the problem.

This thesis proposes three solutions to the above problem. These solutions are: the Hilbert transform technique for DSSS/DQPSK, the Chip Detection technique also for DSSS/DQPSK, and the differential detection for DSSS/BFSK. The first method succeeds in eliminating the BER floor at low processing gains such as 15. However, it fails at higher processing gains. The second method, Chip Detection, is able to correct the problem at all the processing gains investigated in this study. However, the designer has to tolerate some SNR loss.

The performance of the third method is investigated at a processing gain of 254 and it eliminates the BER floor at higher modulation indices ($h \geq 4$) irrespective of the receive bandpass filter.

ACKNOWLEDGMENTS

I would like to thank the following people who encouraged me both at the academic and at the personal level over the last two years.

First of all I would like to thank Dr. Michel Fattouche, my supervisor, whose help, support, encouragement, and good suggestions helped me finish this project on time with a lot of success. Both TRLabs and University of Calgary provided financial support in the form of the TRLabs Graduate Scholarship and the teaching assistantship which I appreciated a lot.

The following people provided valuable insight when I needed them. They are Dr. Abu Sesay, Grant McGibney, Bob Davies, Dr. Brent Petersen, Brian Ebel, Niall Sexton, Saskia Ratzlaff, Mohsen Hosseinian, Danesh Karunnanayake, Andrew Borsodi, and Jason Sokolosky.

Once again, I would like to thank my supervisor, TRLabs, University of Calgary, and all the other people who supported me throughout the last two years.

This thesis is completely dedicated to

my father and my mother who

did everything to educate me

with all the difficulties

they had

TABLE OF CONTENTS

LIST OF TABLES

LIST OF FIGURES

LIST OF SYMBOLS AND ABBREVIATIONS

τ	Arbitrary delay.
f_c	Carrier frequency.
$\delta\phi$	Differential Phase.
$H[\ ]$	Discrete Hilbert Transform operator.
f_{dev}	Frequency deviation.
Ω	Frequency.
H_i	Hilbert Transform operator.
α_p	Information bearing phase.
I_k	Information in phase.
f_d	Maximum doppler frequency.
f_m	Maximum doppler frequency.
h	Modulation index.
μ	Phase bias.
ϕ	Phase.
θ	Phase.
f_s	Signal bandwidth.
λ	Wavelength.
AWGN	Additive White Gaussian Noise.
BER	Bit Error Rate.
BFSK	Binary Frequency Shift Keying.
BW	Bandwidth.
CW	Continuous Wave.
dB	Decibel.
DPSK	Differential Phase Shift Keying.
DQPSK	Differential Quadrature Phase Shift Keying.

DSSS	Direct Sequence Spread Spectrum.
FFT	Fast Fourier Transform
GSC	Golay Sequential Code.
Hz	Hertz.
IF	Intermediate Frequency.
ISI	Inter Symbol Interference.
MaxP	Maximum Phase.
MP	Minimum Phase.
PG	Processing Gain.
PN	Pseudo-Noise sequence.
POCSAG	Post Office Code and Standardization Advisory Group.
s	Second.
SNR	Signal to Noise Ratio.
SS	Spread Spectrum.
SURP	Simulation of the Urban Radio Propagation.
T	Symbol Duration.
T_b	Symbol Duration.
Tc	Chip duration.
VCO	Voltage Controlled Oscillator.

Chapter one

Introduction

1.1 Introduction to paging

Paging is an economical solution to the “all times, all places, all people” communication problem [15]. It started many years ago as a “one bit” messaging system where only a selected number of people can reach a particular pager [3]. Now, it can be categorized as a one-way messaging system over wide areas where a typical pager contains a numeric display to indicate the telephone numbers of the calling party. Hence, this kind of paging system has to rely on the wire-line or the cordless telephone network to complete communication.

This paging system is optimized to take advantage of the asymmetry (one way). Therefore high transmitter towers with several hundred watts to kilowatts are needed to provide the following features at the receiver:

1) Low complexity.
2) Low power consumption.
3) Light weight.
4) Smaller batteries and large usage time.

All of the above plus the efficient use of the RF spectrum provides an economical way of communicating with a person on the move. Hence, the paging system can be used to provide cheap wireless electronic-mail access.

Currently, there are 51 million paging subscribers in the world [10] of which 15 million are in United States. Paging has also become very popular in Asia and is expected to double the current subscriber levels in the next three years. Also, they are freely available. And in some countries, pagers can be bought through mail order or from vending machines.

The coverage of paging systems has increased from local to regional and from regional to nationwide. These vast coverages are usually achieved with multiple transmitters transmitting the same message (simulcasting). However, with the help from network protocols different paging systems can be linked together. This will enable the use of satellites to provide global paging.

1.2 History of Paging

The history of paging goes as far back as 1921 when the Detroit Police department deployed the first land mobile radio system. Paging became popular in the USA in the 1930s where government agencies, police departments, and armed forces used them to broadcast messages from a stationary base station to mobile units.

The concept of wide area paging was first introduced in North America in 1963. The early systems used tones for signaling. Two tones out of several tones were used to identify a pager. If two tones matched a particular receiver's code, it will be alerted. Due to the limited number of pager addresses that this two tone system could support, 5/6 tone format was invented. Up to 12 frequencies were used in this system to represent digits 0 to 9 and a repeat tone R and a special tone X. This format could support up to 100,000 pagers with code numbers from 00,000 to 99,999.

The first binary digital paging scheme was introduced in Canada in 1970. This led to an increased interest in digital paging schemes in Japan, Sweden etc. At the same time (mid 70s), the British Post Office was designing a new paging code and format that would satisfy their requirement. Post Office Code and Standardization Advisory Group (POCSAG) was established for this task. This new paging code, POCSAG, was first published in 1978. Later on, POCSAG and Motorola's Golay sequential code became widely accepted. Also, a much faster protocol FLEX was developed by Motorola.

1.3 Current paging techniques

This section will discuss current paging techniques: 1) POCSAG 2) GSC and 3) FLEX and REFLEX.

1.3.1 POCSAG

POCSAG paging code consists of 16 pager addresses that are batched into 8 time slots (frames). Each of these batches are repeated every 1.0625 seconds. Battery life, code capacity and signaling rate are all optimized in this manner. POCSAG code word is a (31,21) BCH code word and an appended even parity bit. Hence each code word is a 32 bit code word and 16 such code words are concatenated to form 8 frames. This standard supports data rates of 512 or 1200 bits per second. The signaling method is FSK with a frequency deviation of 4.5 kHz. In most cases such signals occupy a channel bandwidth of 25kHz. POCSAG has an address capacity of $8*10^6$.

1.3.2 Golay Sequential Code (GSC)

Motorola's GSC paging scheme is based on the (32:12) Golay code. The signaling method for GSC is FSK with a frequency deviation of 4 kHz [19]. It supports data rates such as 300 bits per second for page addresses and 600 bits per second for messages. Each transmission batch of this method consists of 16 pagers and the transmission sequence contains a preamble and one or more batches. Each paging address consists of two consecutive code words. This method can support a maximum of 409,000 addresses.

1.3.3 FLEX and REFLEX

A high speed paging protocol FLEX was developed by Motorola and is capable of achieving 5 times more capacity than POCSAG 1200. It is also capable of supporting more that 600,000 pagers per channel at the maximum speed. FLEX can be used with a mixture of existing systems such as POCSAG or GSC. A new RF protocol named REFLEX has been designed to provide a reverse channel to support two-way paging. It will allow subscribers to reply to a message or acknowledge, so that the spectrum can be re-used to increase the capacity of the system. Two way paging enables the messaging unit to automatically register the whereabouts of the user. This REFLEX protocol was specifically designed for the Federal Communications Commission's (FCC) Narrowband Personal communications spectrum [10] auctioned in 1994. 930-931 MHz and 940-941 MHz will be used for out bound messages and 901-902 MHz will be used for the in bound messages according to the above frequency allocation.

1.4 Why Spread Spectrum (SS) ?

One of the objectives of paging whether it is one-way or two-way is to transmit signals as far as possible with low bit error rates. In two-way paging more base stations are required to receive the signals rather than to transmit them. This is due to the lack of power at the pager.

A solution to the lack of power at the pager is to increase the energy per information symbol over the reverse channel (i.e. from the pager to the base station) by increasing the symbol duration (i.e. at the cost of reducing the bit rate) for a fixed transmit power. This is particularly feasible since the transmitted packets on the reverse link consist mainly of "ACK" (acknowledge) and "NACK" (negative acknowledge). One can elect to increase the symbol duration directly by repeating the symbol number of times hence, reducing the signal bandwidth. Equivalently, one can use a long PN sequence to replace the information symbol hence preserving the information signal bandwidth. In this thesis we have elected to use DSSS to increase the duration of the information symbol in order to take advantage of its interference rejection capability. One should keep in mind that both techniques have similar performances over the flat fast fading channel.

Since there is only 25 kHz of available bandwidth, urban multipath channel and doppler make SS communication susceptible to an irreducible BER due to the nonstationarity of the channel. In other words, when SS is transmitted over a 25 kHz band, the processing gain provided by SS communications forces the urban multipath channel to behave like a flat fast fading channel, which distorts the differential phase of the signal by the commonly known "Random FM" distortion.

Such a distortion exists regardless of the Signal-to-Noise Ratio (SNR) level and causes bit errors even at high SNR, hence the name 'irreducible BER'.

1.5 What is Spread Spectrum?

SS techniques have been used since world war II [20] for electronic communication. It is a very secure form of communication because the information signal is hidden in a data sequence which is of little importance. The receiver has to know that particular data sequence to recover the information signal. SS provides features such as interference suppression, energy density reduction, and ranging or time delay measurement [22]. Such features are achieved by adding redundancy to the information signal by increasing the information signal bandwidth for a fixed information rate or equivalently, by reducing the information rate for a fixed signal bandwidth.

There are mainly two basic types of SS [20]:

1) Direct sequence.
2) Frequency hopping.

1.6 Direct Sequence Spread Spectrum (DSSS)

This thesis studies only DSSS which can be used with conventional modulation schemes such as Frequency Shift Keying (FSK), Phase Shift Keying (PSK) and differential schemes such as Differential PSK (DPSK), Differential Quadrature PSK (DQPSK) etc. DSSS can be explained with a pictorial representation of signals in both time and frequency.

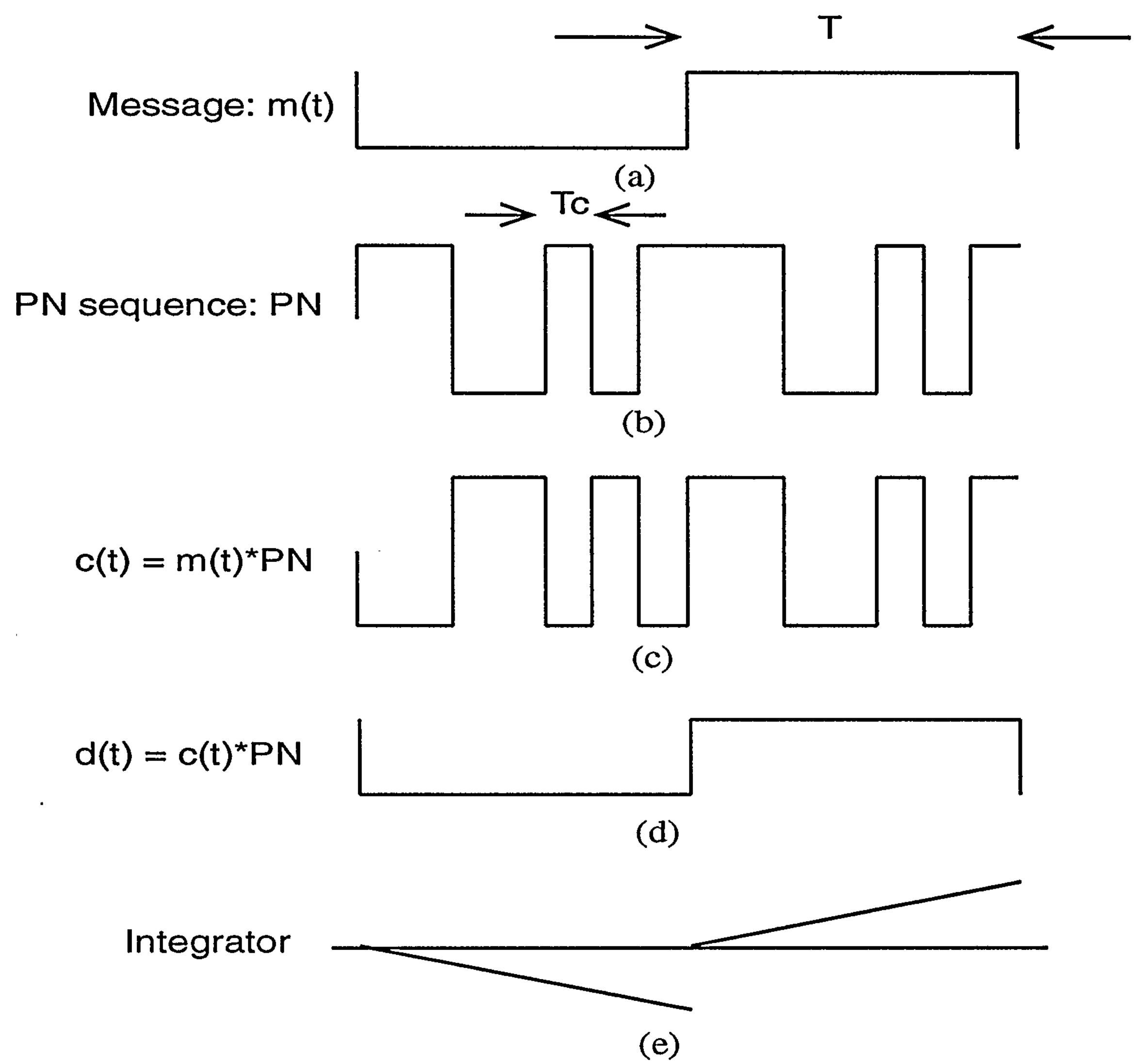

Figure 1.1 DSSS illustration in time domain.

Figure 1.1(a) shows the message, m(t), with a bit duration of time T. Although the spectrum M(f) of m(t) is actually different from the box shown in figure 1.2(a), all the significant frequency components are assumed to be contained in a box of width 1/T. m(t) is first multiplied by the Pseudo-Noise (PN) sequence shown in figure 1.1(b) giving the signal c(t) in figure 1.1(c). The spectrum C(f) of c(t) has an increased bandwidth compared to M(f) as displayed in figure 1.2(b). The smallest entity in the PN sequence shown in figure 1.1(b) is called a chip with a time duration Tc. The signal c(t) is then multiplied by a PN sequence which is exactly the same as in figure 1.1(b) in order to recover the original message (figure 1.1(d)). Finally, an integrator which integrates m(t) over the symbol duration T can be used before the decision stage as shown in figure 1.1(e)

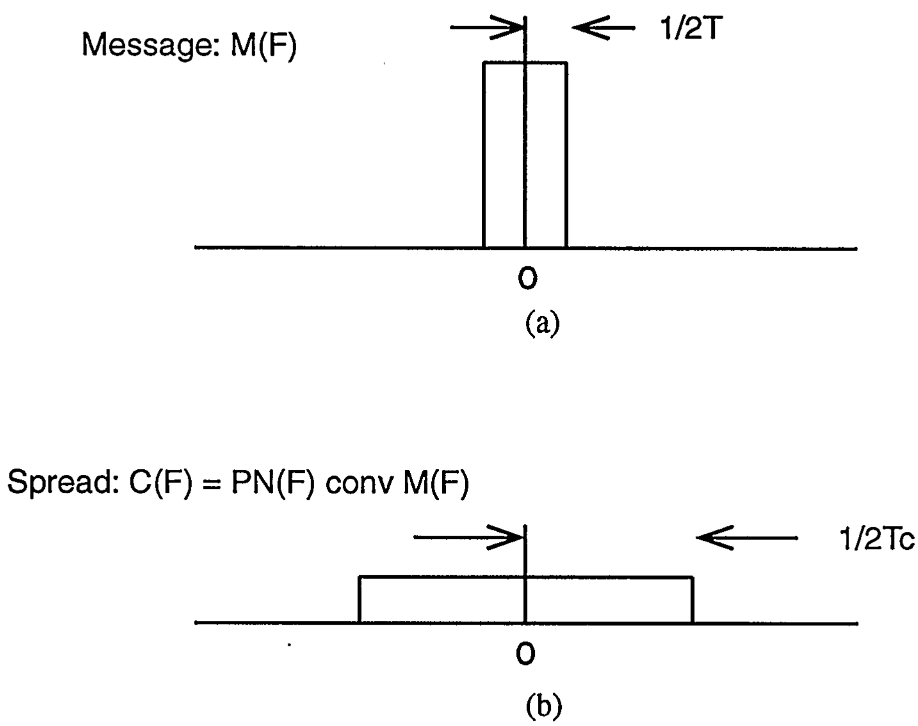

Figure 1.2 DSSS illustration in frequency domain

1.7 Outline of the thesis

Irreducible bit error rates (error floors) occur when data are transmitted over a flat fast fading channel. This problem is discussed in chapter two together with its effects on DSSS. This thesis investigates three different techniques in eliminating the bit error floor. Chapter three introduces the first of such techniques based on the Hilbert transform. Chapter four introduces a novel technique in eliminating the error floor that exists at high processing gains. This technique is called Chip detection because some processing at the chip level is needed to eliminate the error floor. Both of the above techniques use DSSS/DQPSK. The third and final technique is based on Binary FSK and is discussed in chapter five. This technique also benefits from the advantages of DSSS. The last chapter concludes with the advantages, disadvantages and possible future work associated with the three techniques.

Chapter two

The Irreducible Bit error rate problem

2.1 Mobile flat fast fading channel

The envelope of an 840MHz CW signal transmitted over a typical radio (paging) channel is shown in figure(2.1) at a vehicle velocity of 100km/h. Deep fades (i.e. >= 20dB) of the envelope shown in figure(2.1) cause large phase distortions as shown in figure(2.2) where differential phase of the mobile channel is plotted against time.

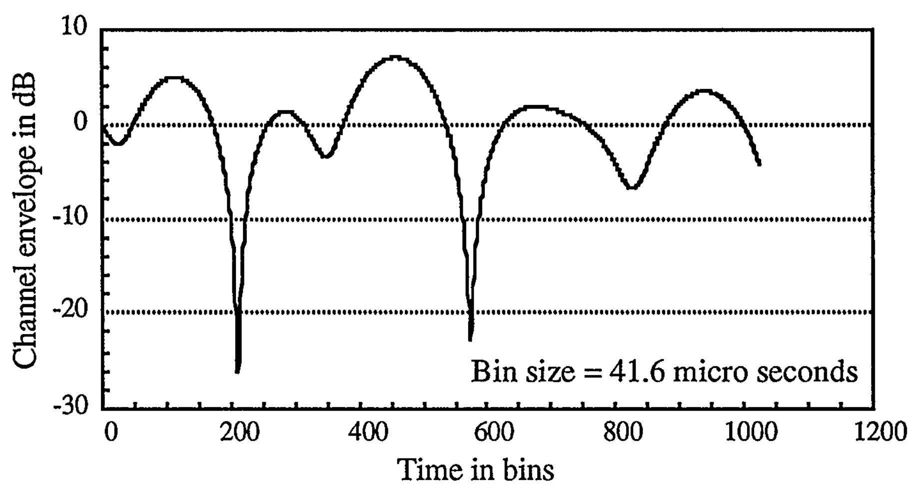

Figure 2.1 Envelope of a CW signal transmitted at a vehicle velocity of 100km/h.

Such channels can be generated using the Modified SURP (Simulation of the urban radio propagation radio channel) program [6]. This program is written in FORTRAN and allows the user to change the vehicle velocity, carrier frequency, symbol rate, number of symbols etc. The Modified SURP program simulates the short term fading more accurately than the original SURP program [9].

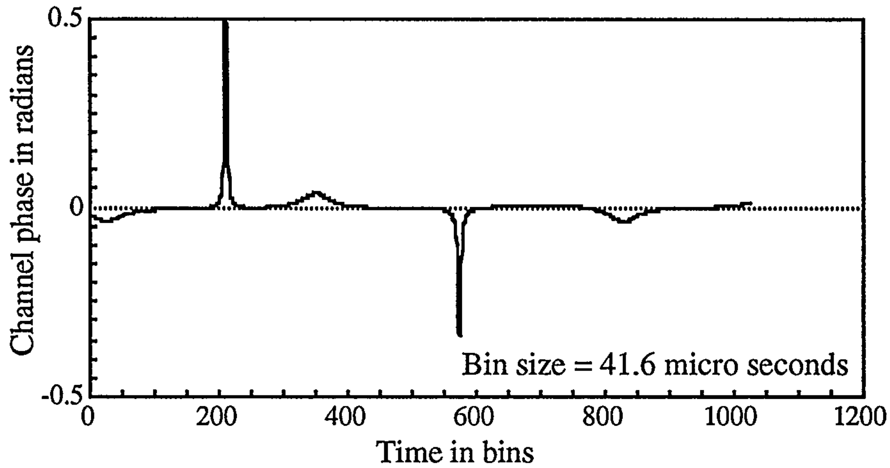

Figure 2.2 Differential phase of the CW signal shown in figure (2.1)

2.2 Irreducible bit error rate

The Phase distortion in figure 2.2 leads to an irreducible bit error rate as shown in curve A of figure(2.4). Curves A, B, and C in figure(2.4) are obtained for the communication system displayed in figure(2.3). This communication system uses DQPSK as the modulation scheme where the information is in the differential phase for a 24ksymbol/sec transmission rate. Hence any kind of phase distortion can create bit errors. In figure (2.4), curve B displays the BER corresponding to an ideal channel where the phase is forced to be constant i.e. having zero differential phase while the envelope is allowed to fade as in figure (2.1). Also, in figure(2.4), curve C illustrates the BER for an AWGN channel demonstrating the well known “Water-fall” curve which is in contrast to the linear curve (curve B).

The performance of the typical communication system is also investigated for lower speeds such as 75km/h and 50km/h for a fixed transmission rate (24ksymbol/sec). Similar BER floors exist at the lower speeds however, with a smaller magnitude as shown in figure (2.5).

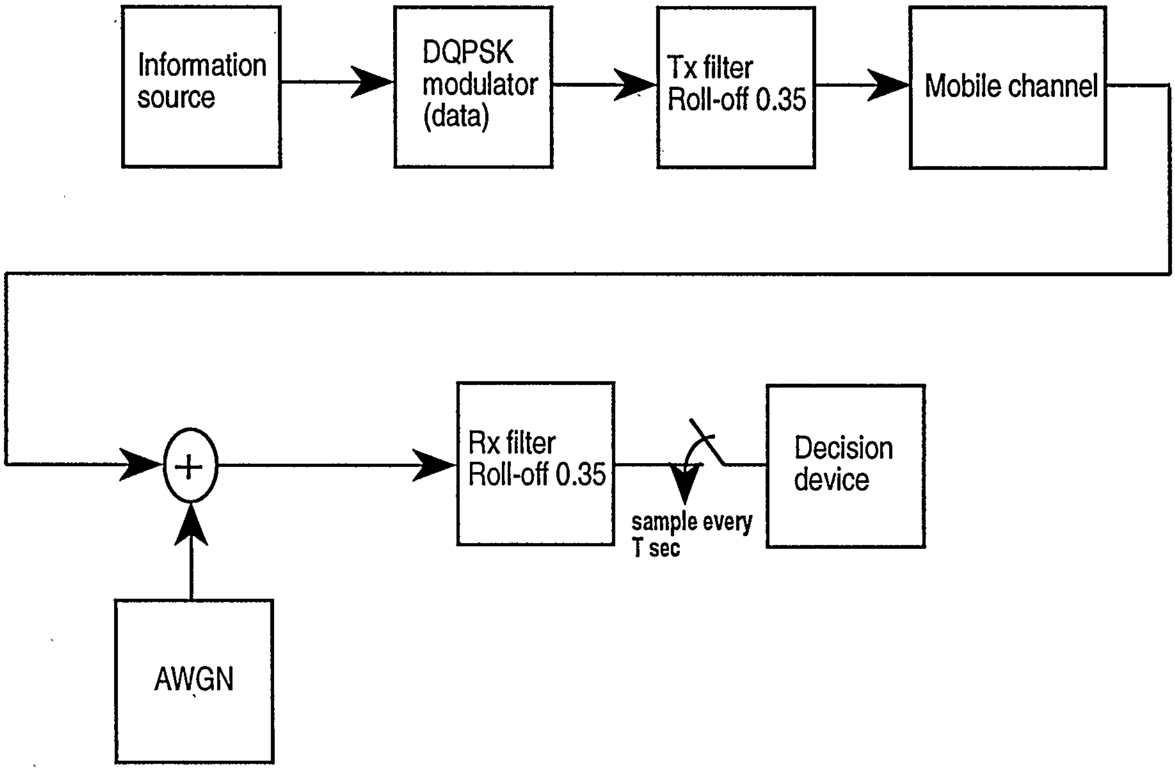

Figure 2.3 Typical DQPSK communication system.

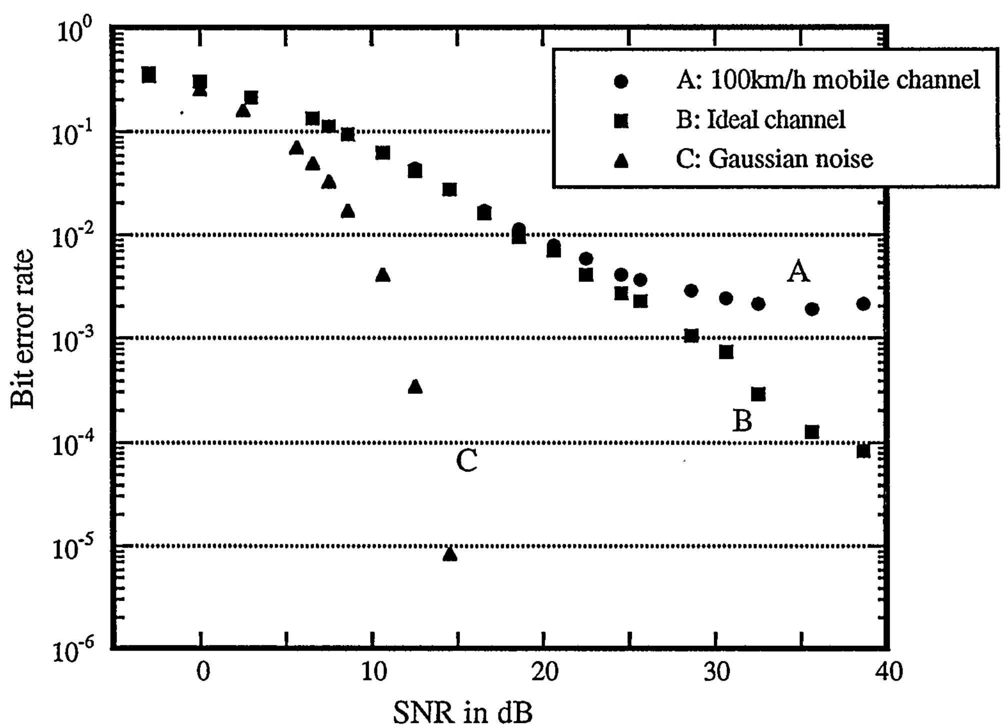

Figure 2.4 BER curves for a typical DQPSK communication system with an AWGN channel, mobile channel, and an ideal channel.

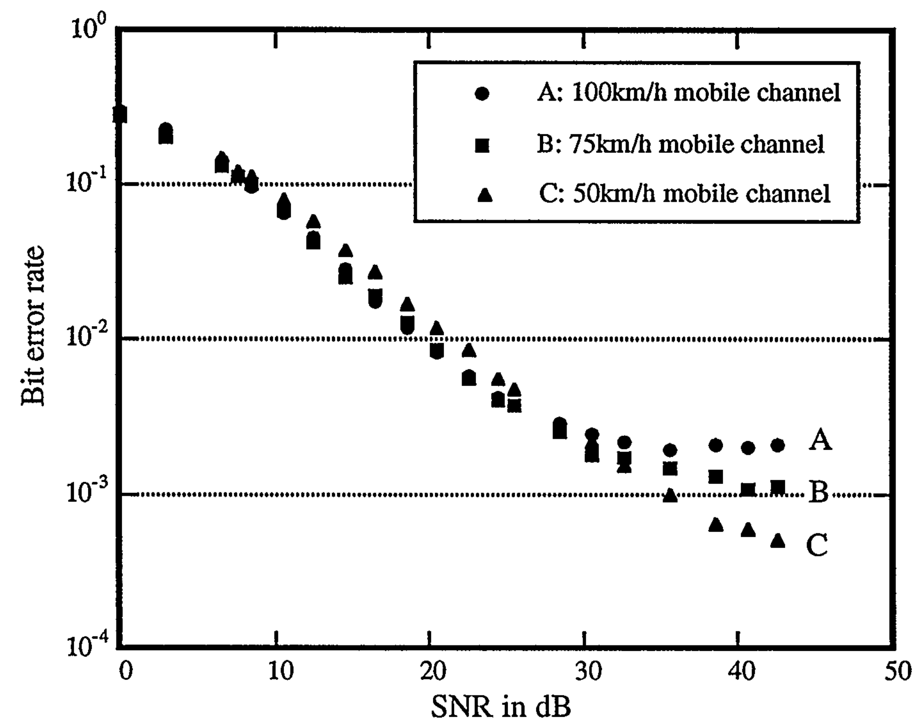

Figure 2.5 BER curves for a typical DQPSK communication system for different vehicle speeds.

2.3 DSSS approach to the BER problem

Figure (2.6) shows the block diagram of a basic DSSS communication system where the DQPSK signal is spread, despread and matched filtered to recover the transmitted information bit. Due to the fixed bandwidth of the mobile channel (25KHz), the information signal bandwidth is always determined by the length of the PN sequence (processing gain). Hence for a processing gain of 15 the information signal bandwidth will be restricted to 1.6KHz, so that it cannot exceed the 24kHz limit when multiplied by the PN sequence (figure (2.7)). Similarly, the information signal bandwidth is limited to 189Hz for a processing gain of 127. For simulation purposes a 24kHz bandwidth is used rather than the 25kHz bandwidth.

The BERs versus SNR at the input of the receiver (i.e. SNR before the correlator) of the DSSS communication system was evaluated in figure (2.8) for processing gains of 15, 31, 63 and 127 at a vehicle velocity of 100km/h. Irreducible BER still exists for all processing gains. However, the problem is more severe for PG=127 (curve A) than for PG=15 (curve D). This is mainly due to the fixed doppler spread that is constant in both cases whereas the information signal bandwidth is much smaller for PG=127 than for PG=15. Figure (2.9) shows the performance of the DSSS communication system at a fixed processing gain of 15. Once again due to increased doppler distortion at higher speeds, the error floor at 100km/h (curve A of figure (2.9)) is $2*10^{-2}$ rather than $6*10^{-3}$ at 50km/h (curve C of figure (2.9)).

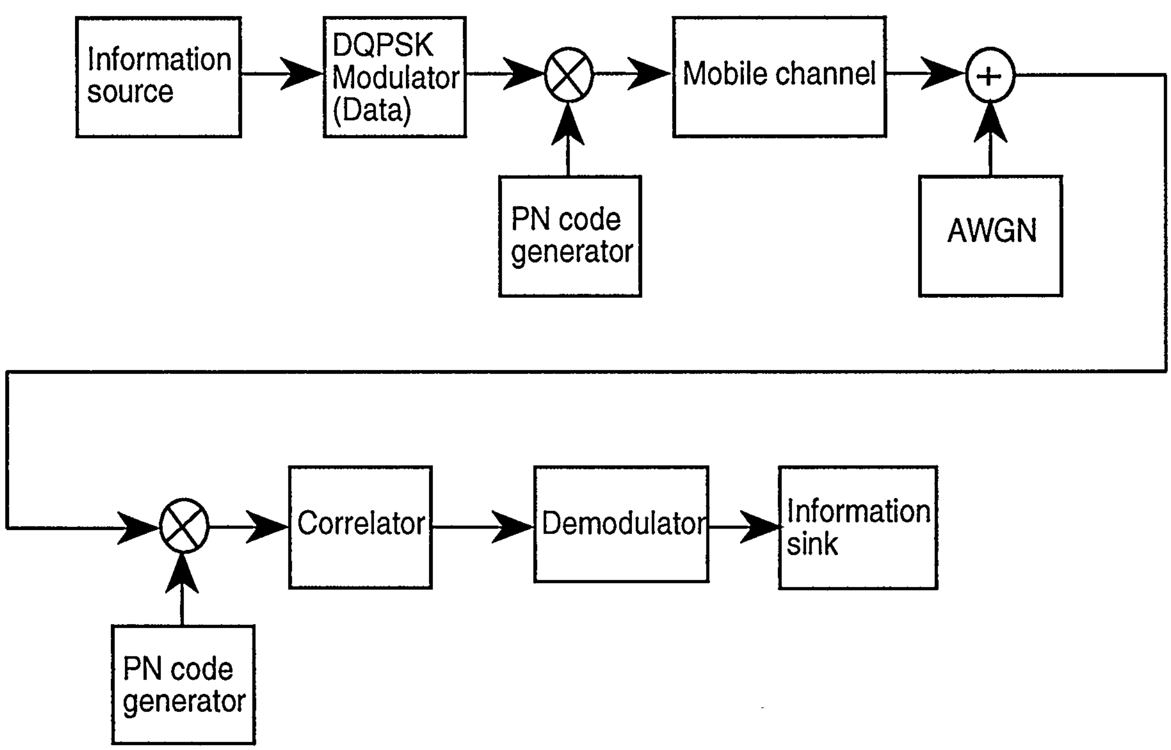

Figure 2.6 DSSS communication system.

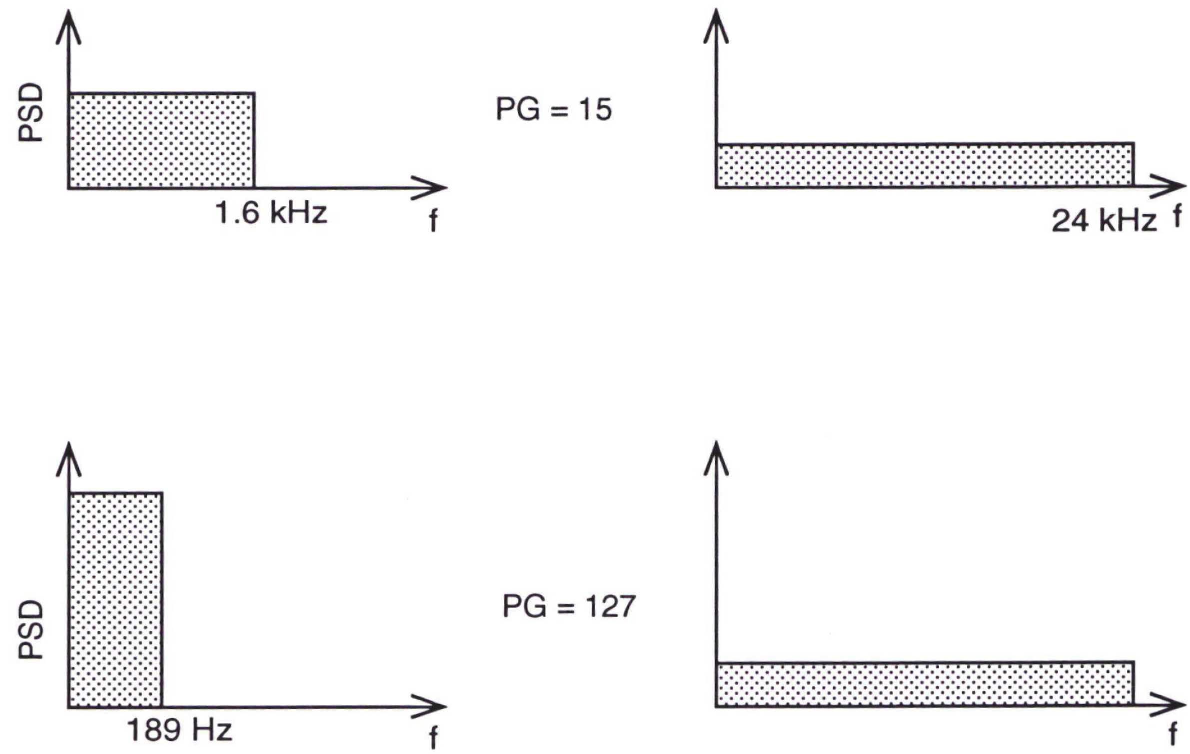

Figure 2.7 Spread spectrum illustration for information signal bandwidth before and after spreading.

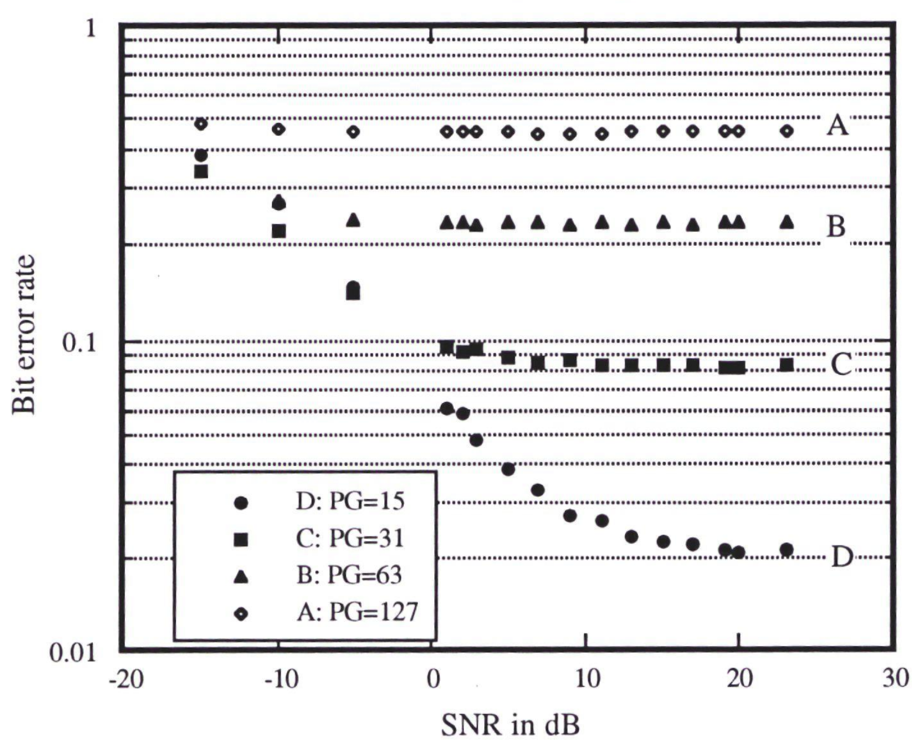

Figure 2.8 BER curves for the mobile channel with different processing gains.

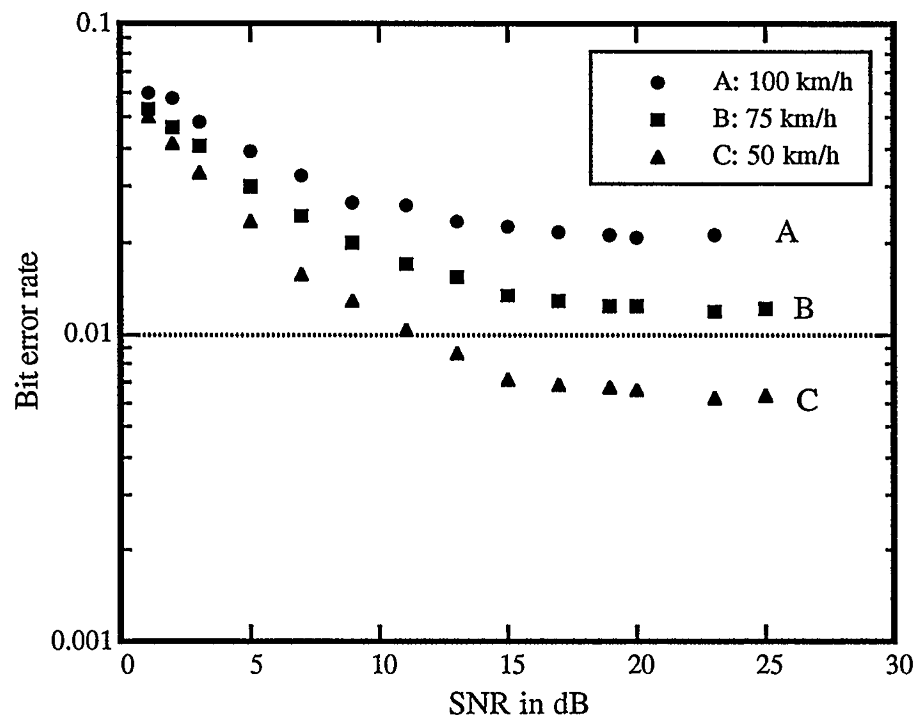

Figure 2.9 BER curves for the mobile channel at different speeds with a fixed PG=15.

The BER floor that exists in the DSSS communication system can be eliminated provided the received signal phase distortion is taken care of. This is evident in figure (2.10) when the same system is used over the ideal channel instead of over the mobile channel with phase distortion. Unlike curves A, B, C, and D of figure(2.8), curves A,B,C, and D of figure(2.10) bend away from possible error floors (towards the y-axis) approaching a “Water-fall” shape at higher processing gains. Such a phenomenon is due to time diversity resulting from a longer information bit duration needed to satisfy the processing gain for a limited channel bandwidth. Hence increased bending is obtained at higher processing gains (curve A in figure(2.10)). Therefore, all the solutions to the irreducible BER problem discussed in this thesis maintain the structure of the basic DSSS system, figure(2.6), except for the additional phase correction block or the modulation scheme.

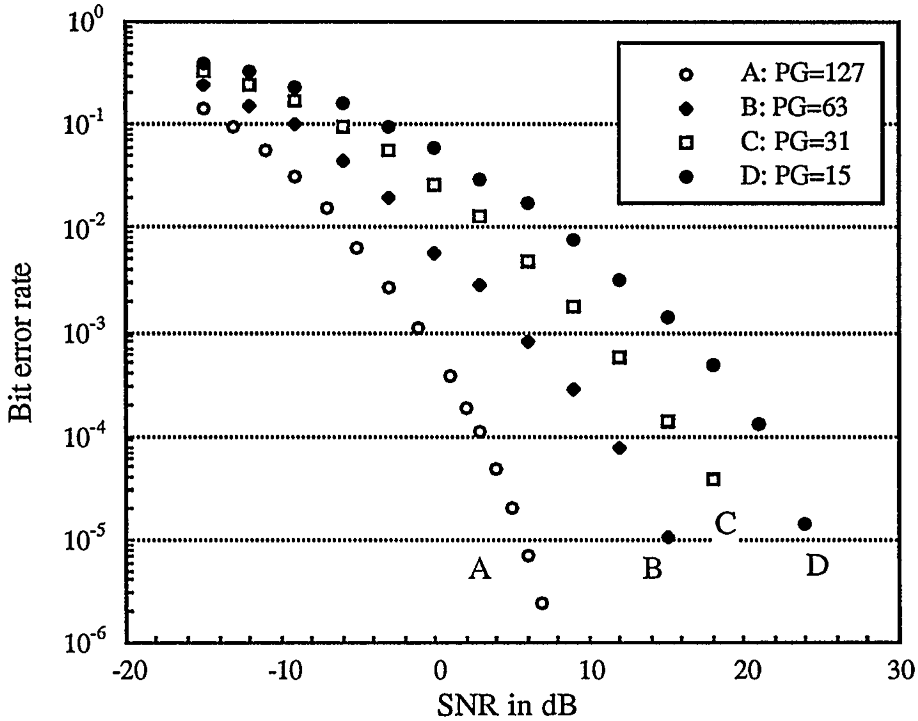

Figure 2.10 BER curves for the ideal channel with different processing gains.

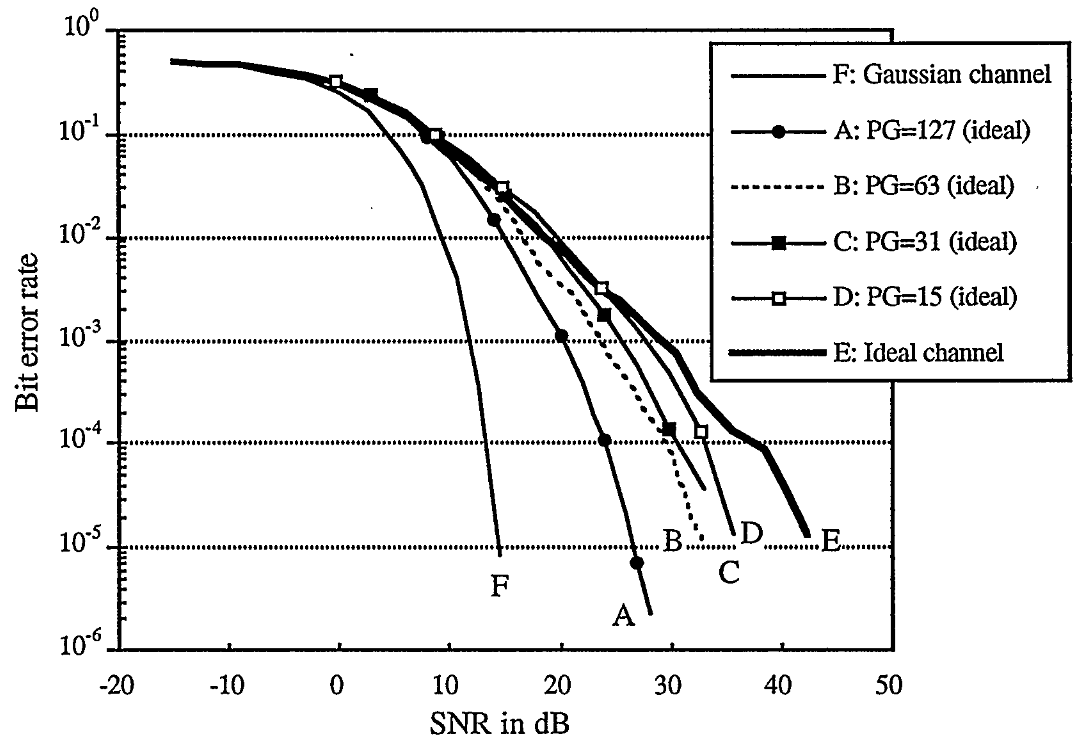

Figure 2.11 Comparison of the DQPSK/DSSS communication system with the typical DQPSK communication system.

In figure (2.11), the BER curves A, B, C, and D of figure (2.10) are illustrated versus SNR after the correlator in figure (2.6). They are compared with the bit error rate curves obtained with the typical DQPSK communication system shown in figure (2.3). The straight line curve E in figure (2.11) is obtained with the typical DQPSK communication system when the channel is ideal whereas the curve F in figure (2.11) is also obtained with the same communication system, however, for a Gaussian channel. From figure (2.11) one can conclude that processing gain 127 offers the largest time diversity among all processing gains considered. This should not be surprising since one can expect one fade every 155 chips at a velocity of 100km/h

2.4 DSSS over the Reverse Link of a Paging System

If phase distortion due to fast fading can be removed, DSSS can provide reliable communications over the reverse link of a paging system where power is at a premium. For instance the following power budget calculation indicates an available path loss of 146dB.

Transmit power	10mW or 10dBm
Required SNR at the input of the receiver	6dB
Noise figure at the receiver (approximately)	10dB
Noise over 189Hz	-152dBm
--	--------------
Affordable path loss	146dB

In the above calculation, it is assumed that the transmitter power is small (10mW) as well as the information bandwidth (189Hz). Such a bandwidth corresponds to a DSSS system with a processing gain of 127 which spreads the 189Hz over a bandwidth of 24kHz. In other words, the noise contribution at the decision device is band limited to 189Hz which is 127 times smaller than 24kHz. As shown later, DSSS over a flat fast fading channel can be regarded as a form of time diversity which approaches the performance of the AWGN channel as the PG is increased. For this reason, a 6dB SNR is sufficient to achieve a 10^{-5} BER at the receiver as seen from curve A in figure (2.10).

On the forward link, the total noise contribution is 127 times larger than the reverse link since the DQPSK signal is not spread before transmission. Furthermore, the transmitter power can be much larger (e.g. 10kW typically) and the signal suffers from flat fading. In other words, a fading margin is required. The following power budget calculation indicates an available path loss of 145dB.

Transmit power	10kW or 70dBm
Required SNR at the input of the receiver	45dB
Noise figure at the receiver (approximately)	10dB
Noise over 24kHz	-130dBm
--	--------------
Affordable path loss	145dB

The 45dB SNR at the receiver corresponds to a 10^{-5} BER as seen from curve B in figure (2.4). In a Nonline-of-sight environment with power law of 4 a path loss of 145dB corresponds to about 1km of transmission at 840MHz.

Chapter three

Hilbert transform based communication system

3.1 What is the Hilbert transform?

The spectrum of a real valued signal $u(t)$ is even, i.e. $U(j\Omega) = U^*(-j\Omega)$ where $U(j\Omega)$ is the Fourier Transform of $u(t)$. Hence it is somewhat redundant to have the same information in the positive and the negative parts of the spectrum. The Hilbert transform can be used to eliminate such a redundancy by eliminating one of the two side bands of the real valued signal. This is referred to as Single Side Band modulation (SSB) which is commonly used in frequency division multiplexing. Figure (3.1a) shows the magnitude $|U(j\Omega)|$ of a real-causal signal $u(t)$. Figure (3.1c) shows $|Y(j\Omega)|$ which is obtained when $|U(j\Omega)|$ is multiplied by the filter response $|H(j\Omega)|$, in figure (3.1b) where

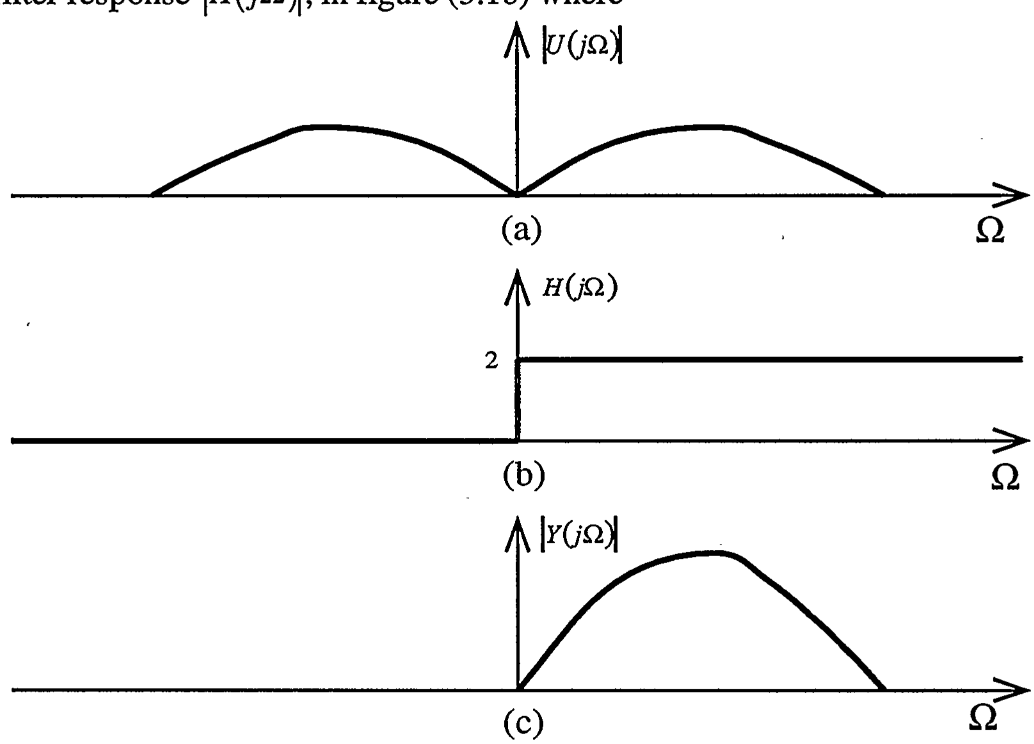

Figure 3.1 Hilbert transform filtering in the frequency domain

$$H(j\Omega) = \begin{cases} 2 & \Omega > 0 \\ 0 & \Omega < 0 \end{cases} \tag{3.1}$$

Since $Y(j\Omega)$ is one sided with only positive frequencies, $y(t)$ is complex in the time domain. Such signals are termed "analytic". An analytic signal has the special property that its imaginary part is related to its real part through a Hilbert transform, i.e.

if $\quad y(t) = p(t) + jq(t) \quad (3.2)$

and $\quad q(t) = H_i[p(t)] \quad (3.3)$

then $y(t)$ is analytic, where H_i is the Hilbert transform operator and $p(t)$ and $q(t)$ are the real and imaginary parts of $y(t)$ respectively.

Taking the inverse Fourier transform of $H(j\Omega)$ we obtain [16]

$$h(t) = \delta(t) + \frac{j}{\pi t} \tag{3.4}$$

With $u(t)$ as the input to the filter $h(t)$, the output of the filter $y(t)$ is obtained as

$$y(t) = u(t) * h(t) = u(t) + j[u(t) * h_i(t)] \tag{3.5}$$

where $h_i(t)$ is the imaginary part of $h(t)$ and '*' denotes a convolution operation,

i.e. $\quad h_i(t) = \dfrac{1}{\pi t} \quad t \neq 0 \quad (3.6)$

The real part of equation (3.5) is simply the original signal $u(t)$, while the imaginary part is obtained by passing $u(t)$ through $h_i(t)$. The Fourier transform of $h_i(t)$ can be easily found using equation (3.1) as follows [18]:

$$H_i(j\Omega) = \frac{1}{2j}\left[H(j\Omega) - H^*(-j\Omega)\right] \tag{3.7}$$

i.e. $\quad H_i(j\Omega) = \begin{cases} -j & \Omega > 0 \\ j & \Omega < 0 \end{cases} \quad (3.8)$

Therefore, $h_i(t)$ can be described as an allpass function that provides a $\frac{\pi}{2}$ phase shift at all frequencies. The above analysis is described for continuous signals. The analysis for the discrete case follows in a similar manner.

3.2 Voelcker's phase envelope relationship

Voelcker in [23] showed that the envelope and the phase of an analytic signal $m(t)$ are related by the following equation:

$$\frac{d\phi(t)}{dt} = H_i\left[\frac{d\left[\ln(|m(t)|)\right]}{dt}\right] \tag{3.9}$$

In [5] Fattouche and Zaghloul estimated the absolute value of the phase differential of a CW signal transmitted over a mobile radio channel using equation (3.9) where $|m(t)|$ is the envelope of $m(t)$ and $\phi(t)$ is its phase. In [7] they showed that the distorted differential phase of an IS-54 signal can be corrected to eliminate BER floors caused by flat fading at a mobile receiver traveling at 100km/h. Since the bandwidth of the signal is fixed at 24.03 kHz and the carrier frequency is around 840MHz (corresponding to $\lambda = 35.7\,\text{cm}$) the signal will fade every 6.4ms (i.e. every $\frac{\lambda}{2}$ at 100km/h). This also means that every 155 symbols the signal experiences a fade which is evident from figure (2.1).

For the discrete case equation (3.9) can be re-written as:

$$\delta\phi_k = H\left[\ln|m_k| - \ln|m_{k-1}|\right] \tag{3.10}$$

where $m_k = m(kT_0)$, $\delta\phi_k = \phi_k - \phi_{k-1}$, and $\phi_k = \phi(kT_0)$. T_0 is the sampling interval and $H[\ ]$ is the discrete Hilbert transform operator.

Figure (3.2) shows the received differential phase ($\delta\phi_k$) and the estimated differential phase ($\delta\hat{\phi}_k$) of the CW signal shown in figure (2.1) obtained using (3.10) with $T_0 = 41.6\mu\text{s}$. As seen in figure (3.2), equation (3.10) estimates $\delta\phi_k$ with a sign ambiguity. This is explained as follows. Near a fade the signal can either be 'locally' minimum phase (MP) or 'locally' Maximum phase (MaxP) depending on whether the zero is inside the unit circle or outside it in the Z-plane [7,5]. If the signal is MP, equation (3.10) accurately determines the sign of $\delta\phi_k$, however, if it

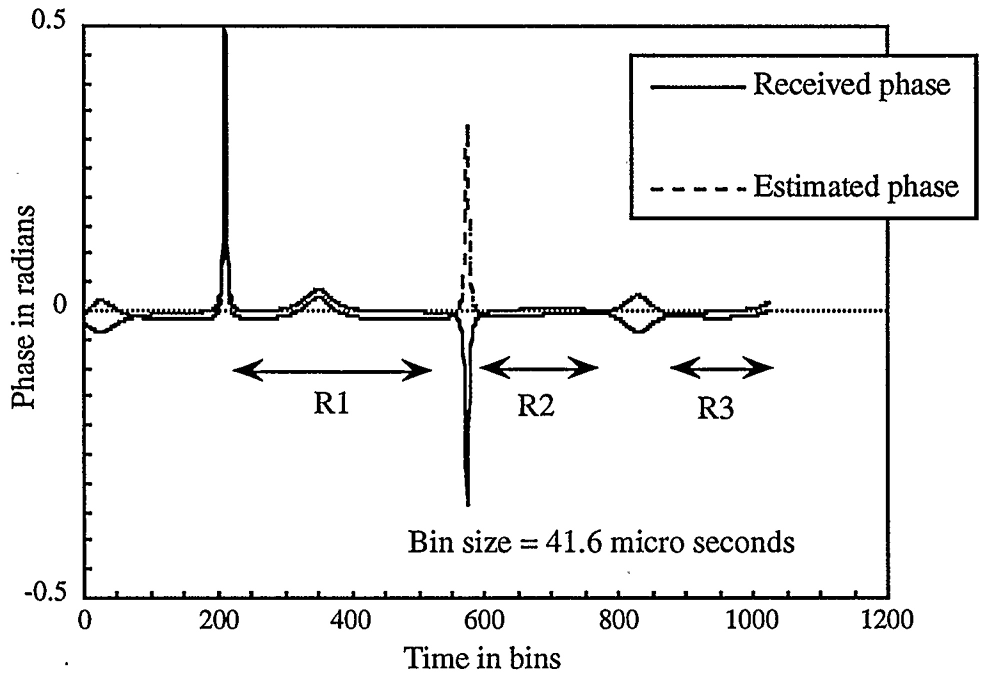

Figure 3.2 Received differential phase and the Hilbert transform estimate of the differential phase.

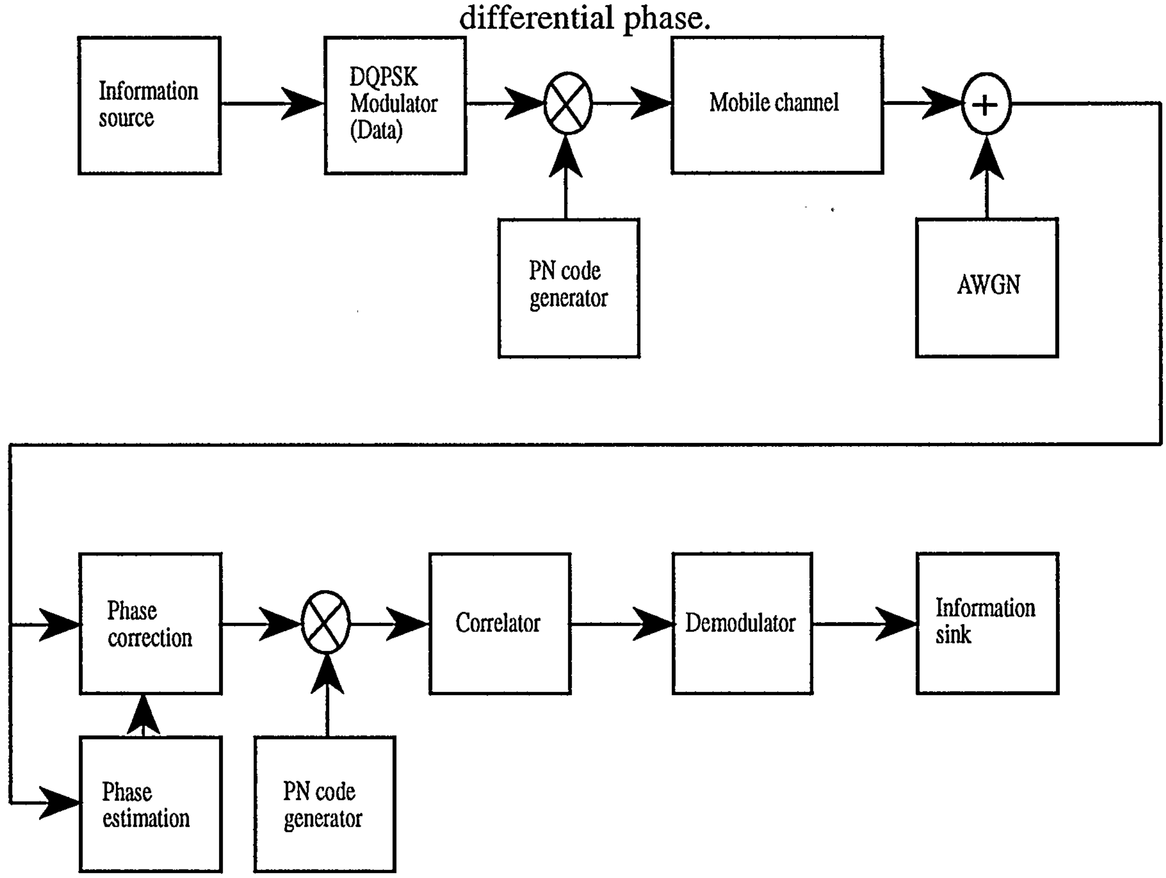

Figure 3.3 DSSS communication system with Hilbert transform.

is MaxP equation (3.10) estimates $\delta\phi_k$ with an opposite sign. This sign ambiguity can be removed as shown in detail later in this chapter.

3.3 Hilbert transform based communication system

Figure (3.3) shows the block diagram of the communication system that is evaluated in this chapter. This system uses DQPSK to modulate the information bits into symbols and Direct Sequence to spread the information symbols. First, information is generated in a binary form at a predetermined rate which is calculated according to the processing gain (PG) of the DSSS PN code and the available channel bandwidth. Then the bits are modulated into DQPSK symbols and multiplied by a PN sequence of an appropriate length in order to generate a wide band SS signal which occupies the entire bandwidth of the channel. The SS signal is then transmitted over a mobile channel which is simulated using stored "inphase" and "quadrature" files generated by the modified SURP program [6]. These files contain the lowpass equivalent of an 840MHz CW signal transmitted over a mobile channel. Additive White Gaussian noise (AWGN) is then added to the spread DQPSK signal after being transmitted over the mobile flat fading channel.

3.4 Eliminating phase ambiguity and distortion

The following steps explain how the Hilbert transform can be used to remove the distorted differential phase due to fades.

1) The "Phase estimation" block in figure (3.3) uses the natural logarithm of the received signal envelope, $ln|m_k|$ and equation (3.10) to obtain $\delta\hat{\phi}_k$, the estimate of $\delta\phi_k$.

The following steps are performed at the "Phase correction" block.

2) Using the received signal envelope the location of each signal fade is estimated as follows. A fade starts when the signal envelope drops more than 3 dB below the average signal envelope and it ends when the signal envelope is less than 3 dB below the average signal envelope.

3) Assuming from step 2) that the signal fades from sample N1 to sample N2 then the sign ambiguity can be resolved as follows. $\delta\phi_k$ may contain a phase bias μ which is not included in (3.10), i.e. $\delta\hat{\phi}_k$ in step 1) will not contain a bias. Instead μ can be calculated by

$$\mu = \frac{1}{N} \sum_{k \in \mathrm{R1, R2, R3}} \phi_k - \phi_{k-1} \tag{3.11}$$

where regions R1, R2, and R3 are non fading regions as shown in figure (3.2). This phase bias can be taken into account by adding μ to $\delta\hat{\phi}$.

4) Calculate S_+ and S_-:

$$S_+ = \sum_{k=N1}^{N2} \min_{p \in \{0,1,2,3\}} \left\{ (\phi_k - \phi_{k-1}) + \left(\delta\hat{\phi}_k + \mu\right) - \alpha_p \right\}^2 \tag{3.12}$$

$$S_- = \sum_{k=N1}^{N2} \min_{p \in \{0,1,2,3\}} \left\{ (\phi_k - \phi_{k-1}) - \left(\delta\hat{\phi}_k + \mu\right) - \alpha_p \right\}^2 \tag{3.13}$$

where $\alpha_p = \frac{p\pi}{2}$ is the information bearing phase and $p \in \{0,1,2,3\}$.

5) If $S_+ < S_-$, $\left(\delta\hat{\phi}_k + \mu\right)$ is added to $(\phi_k - \phi_{k-1})$, otherwise $\left(\delta\hat{\phi}_k + \mu\right)$ is subtracted from $(\phi_k - \phi_{k-1})$.

Step 5) removes the distorted differential phase that exists between symbols N1 and N2. After that the signal is multiplied by the same PN sequence as before followed by the "Correlator" where the signal is integrated over the symbol period T_b. The output of the correlator is demodulated into bits using a decision device.

3.5 Performance of the Hilbert transform based communication system

BER curves obtained through simulation of the communication system in figure(3.3) are displayed in figures 3.4 to 3.8 for a mobile channel bandwidth of 24.03kHz, a carrier frequency of 840MHz and a vehicle velocity of 100km/h.

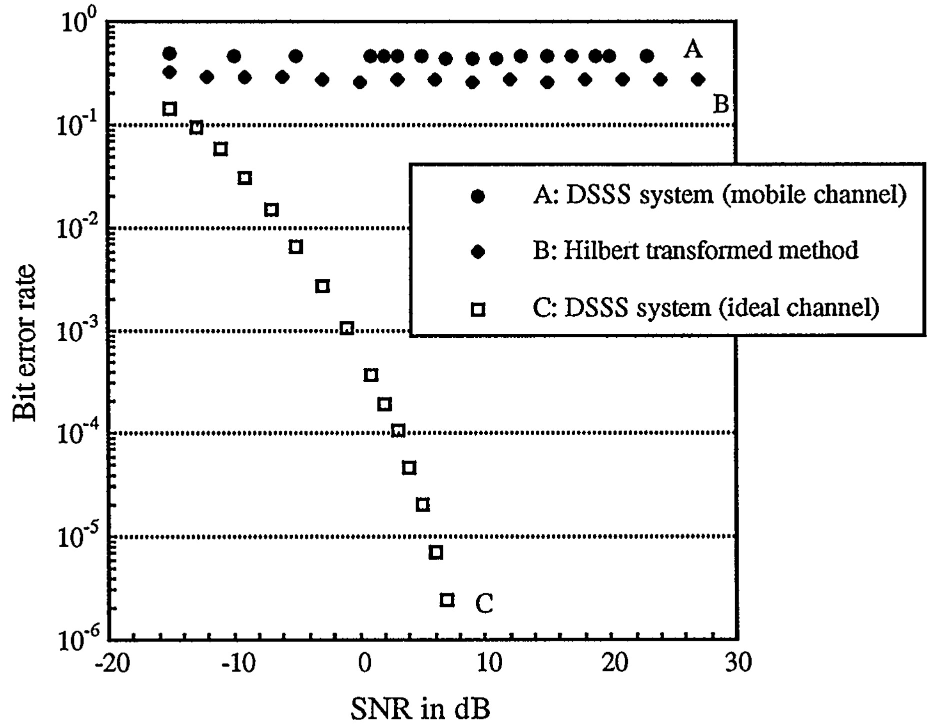

Figure 3.4 BER curves for the Hilbert transform based communication system and the DSSS communication system for PG=127.

In figure (3.4) three BER curves are displayed for a PG = 127. Curve A in figure (3.4) is obtained using a conventional DSSS communication system (without phase correction). Curve B is obtained for the communication system discussed in this chapter (figure (3.3)). BER of both curves display error floors (irreducible BER) at all SNRs (-15dB to 27dB) investigated here. However, the BER curve for the ideal channel, where the differential phase distortion is forced to be constant while the envelope is allowed to fade, performs as well as the well known "Water-Fall" curve of an unfaded AWGN channel. Hence, the system shown in figure(3.3) fails to eliminate the BER floor.

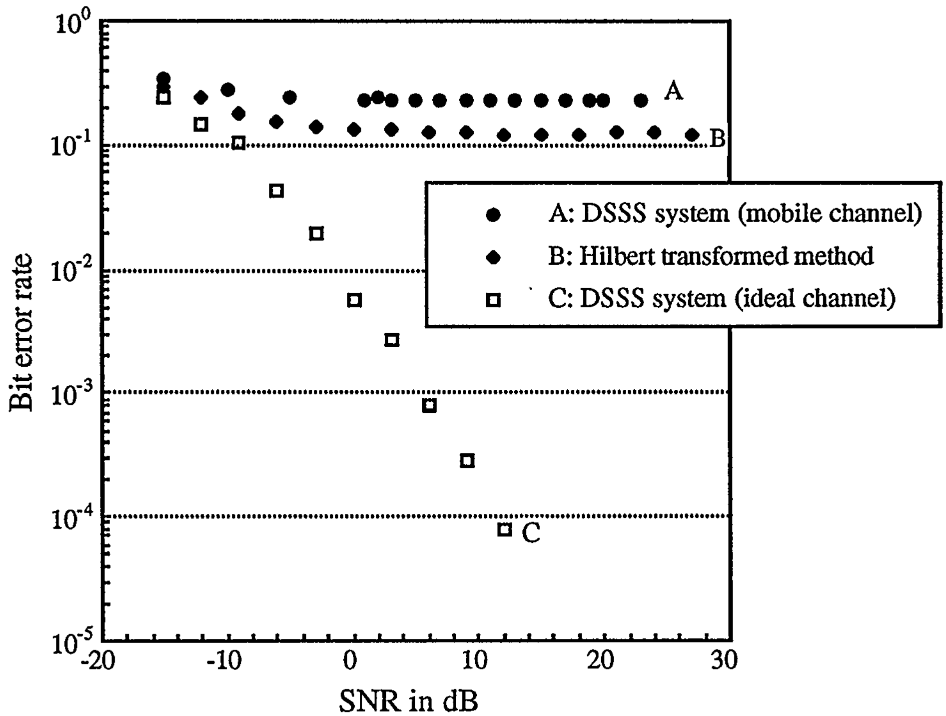

Figure 3.5 BER curves for the Hilbert transform based communication system and the DSSS communication system for PG=63.

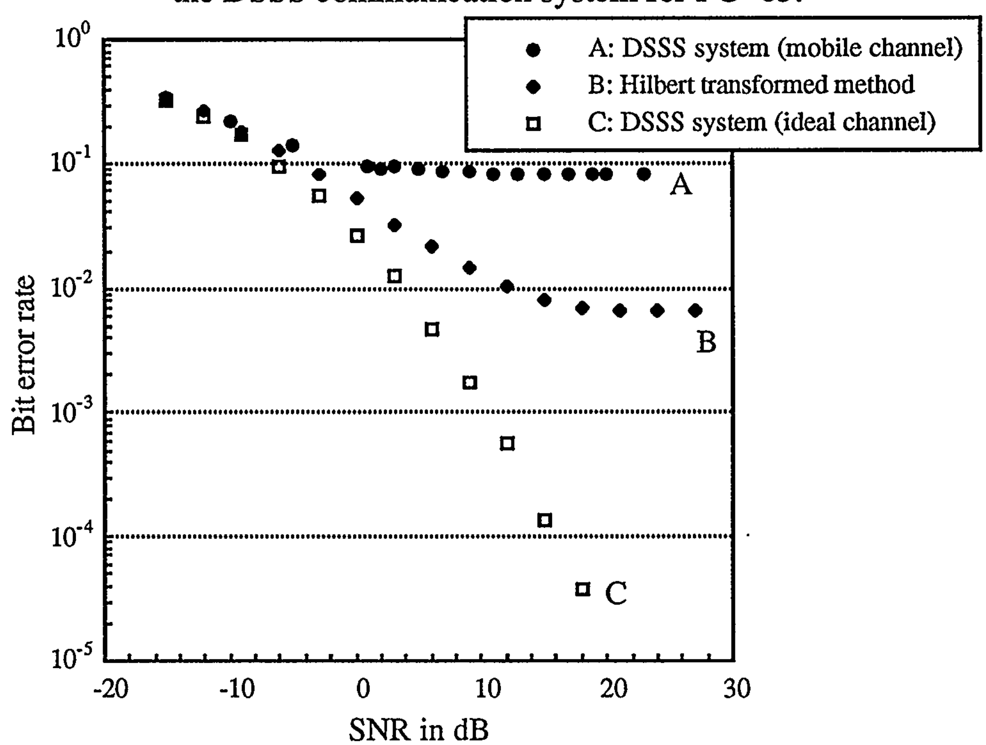

Figure 3.6 BER curves for the Hilbert transform based communication system and the DSSS communication system for PG=31.

In figure (3.5) three BER curves are displayed for a PG = 63. Curves A, B, and C in figure (3.5) are obtained for similar conditions as figure(3.4) except for the smaller processing gain. Once again curves A and B show BER floors.

In figure (3.6) three BER curves are displayed for a PG = 31. In this case the BER floor of curve A is at 0.1, however, curve B (with the Hilbert transform correction) shows some improvement with an error floor lower than 0.01. Compared with curve B from previous figures (3.4 and 3.5), curve B in figure (3.6) shows an improvement of at least 10 times to the BER floor.

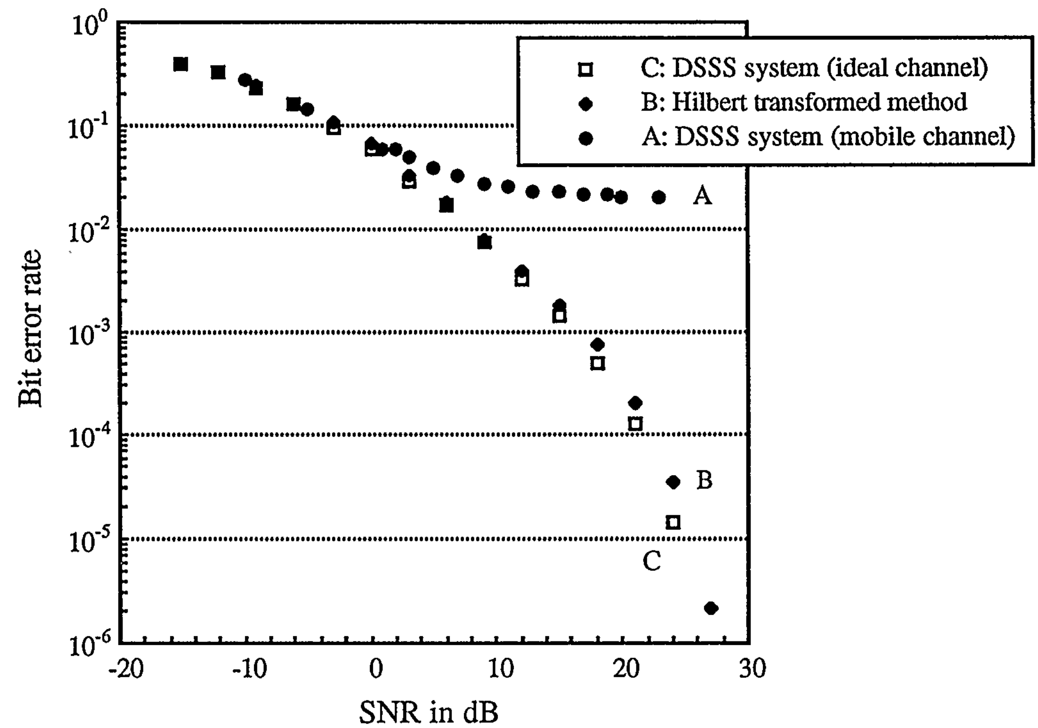

Figure 3.7 BER curves for the Hilbert transform based communication system and the DSSS communication system for PG=15.

In figure (3.7) three BER curves are displayed for a PG = 15. In this case the irreducible BER of curve A is eliminated in curve B and it approximates the performance of the ideal curve (curve C). Both curve B and curve C bend away from curve A giving desirable results at high SNRs of 20dB or more. Hence, a processing gain of fifteen is optimum for this method when the vehicle velocity is 100km/h.

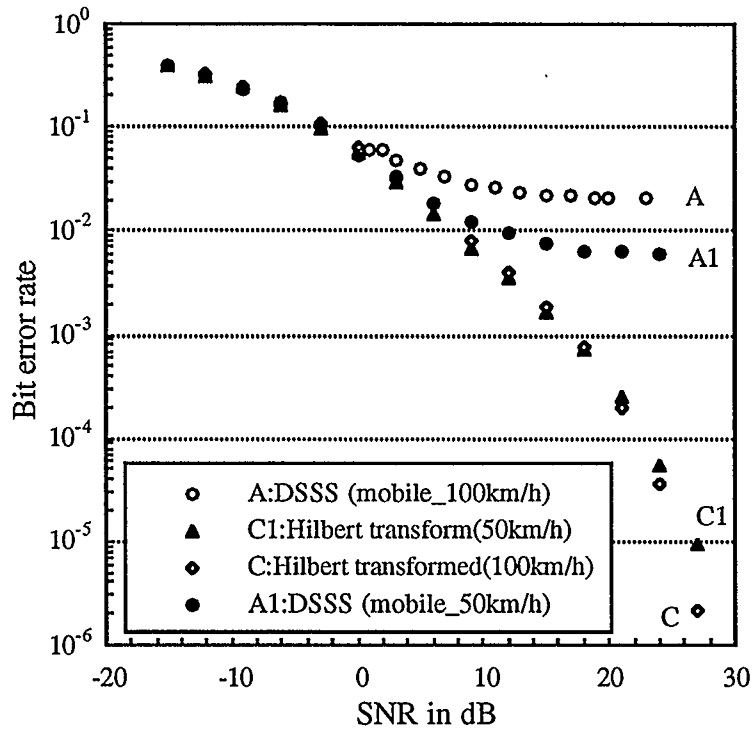

Figure 3.8 Performance of the Hilbert transform based communication system compared to the DSSS communication system for PG=15.

In figure (3.8) four BER curves are displayed for a PG = 15. Two curves (curves A and C) correspond to a vehicle velocity of 100km/h while the remaining two curves (curves A1 and C1) correspond to a vehicle velocity of 50km/h. As expected, curve C1 demonstrates that the system is capable of eliminating the BER floor that exists at 50km/h (curve A1). However, for the same system, curve C performs better than curve C1 at SNRs of 20dB or above. This is due to the fact that at high speeds (100km/h) the vehicle passes through a signal fade faster than at slower speeds (50km/h).

3.6 Concluding Remarks

In this chapter, a Hilbert based method was used in an attempt to eliminate the BER floor associated with the transmission of a DQPSK/DSSS signal over a mobile urban channel. The attempt failed at high processing gains (PG = 31, 63, 127,...) when the mobile velocity is 100km/h or more. In the next chapter, an alternative method is introduced in an attempt to eliminate the same problem.

Chapter four

Communication system with chip detection

4.1 Why an alternative technique?

It is evident from figure(3.4) that the performance of the Hilbert transform based communication system as described in figure(3.3) is not satisfactory at high processing gains (PG = 31, 63, 127, ...) when the mobile velocity is 100km/h or above. The reason for the poor performance is that at high processing gains, the information rate (before spreading) is of the order of the maximum doppler frequency f_d. For instance at a processing gain of 127 the information bandwidth is 189Hz (figure(2.7)) and the maximum doppler frequency, f_d, for an 840MHz carrier can be calculated as follows:

$$\text{Since } \lambda = \frac{c}{f} = \frac{3*10^8}{840*10^6} = 35.7\text{cm} \tag{4.1}$$

$$\text{then } f_d = \frac{\textit{mobile velocity}}{\lambda} = \frac{27.78\text{m/s}}{0.357\text{m}} = 77.78\text{Hz} \tag{4.2}$$

Figure (4.1) shows the doppler spectrum of the radio channels used in the simulations and the maximum doppler spread according to figure (4.1) is about 80Hz. Hence, the calculated value of the doppler spectrum given by equation (4.1) agrees with figure (4.1). Since the effect of the flat fast fading channel on the signal is to spread its spectrum over the doppler spread, one should expect a poor performance when the signal spectrum is comparable with the width of the doppler spread. This is particularly evident when using FSK as shown in Chapter five.

Hence at high processing gains the distortion due to the doppler spread is severe relative to the information bandwidth. Also, regions [R1, R2, and R3] in figure(3.2) show some offset between the estimated differential phase and the received differential phase of the signal due to doppler. These offsets will not be corrected by the Hilbert transform based system. Only severe phase distortions due to large fades will be removed by such a system while the small offsets accumulate over the duration of one PN sequence. Thus, the longer the PN sequence the larger the accumulation.

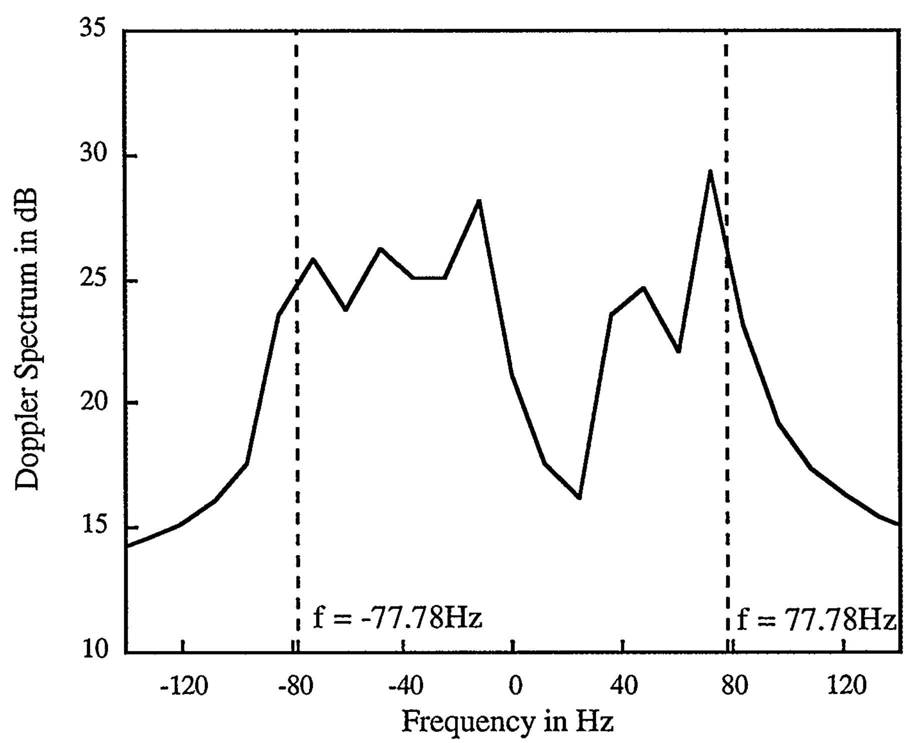

Figure 4.1 Doppler spectrum of the channels used in simulations.

4.2 Chip detection technique

A new method, called chip detection, is introduced in this chapter in an attempt to eliminate the above problem. The theoretical explanation for such a method is shown below. The DQPSK modulation scheme is used with the following encoding and decoding process at the transmitter and at the receiver.

4.2.1 Transmitter differential encoding:

At the nth chip,

$$\phi_n = \phi_{n-1} + I_k + \theta_n \qquad \text{for } nTc < t < (n+1)Tc \quad (4.3)$$

where ϕ_n is the phase of the nth chip and I_k is the information phase $\in \left(0, \frac{\pi}{2}, \pi, \frac{3\pi}{2}\right)$. θ_n is the phase of the spreading PN sequence (i.e. π and 0).

The symbol is decoded and then despread at the receiver as follows.

4.2.2 Receiver differential detection for each chip:

Decoding: $\psi_n = \phi_n - \phi_{n-1} = I_k + \theta_n$ (4.4)

Despreading: $\psi_n + \theta_n = I_k + 2\theta_n = I_k;$ (4.5)

assuming a noise-free channel without distortion.

Note that, $2\theta_n$ can take only values of zero or 2π. Therefore, the information can be recovered from equation (4.5) after passing it through a matched filter. However, an extra chip is needed to be transmitted with each symbol to be used as a reference chip. Hence, 16 chips are required to be transmitted for each symbol at a processing gain of 15.

4.3 Communication system with chip detection

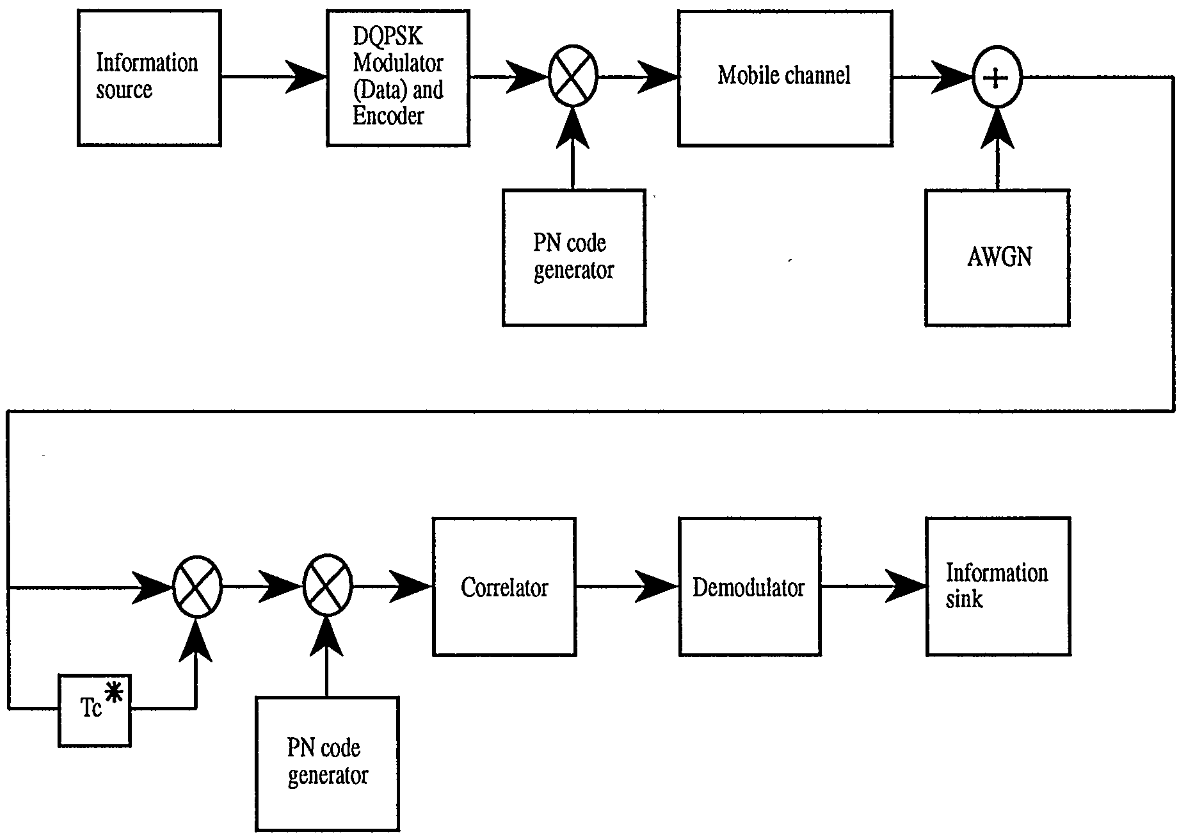

Figure 4.2 Communication system with chip detection.

The communication system designed with equations (4.3), (4.4), and (4.5) is shown in figure (4.2). Once again the information is generated at a pre-calculated rate that depends on the channel bandwidth and the processing gain (figure (2.7)). The information bits are DQPSK modulated and differentially encoded according to equation (4.3). They are then spreaded with the desired PN sequence and passed through the mobile channel generated from the modified SURP package. AWGN is added after the channel. This system is different from the Hilbert transform based communication system in figure (3.3) since a multiplier and a delay unit are used here instead of the "phase estimation" and "phase correction" blocks. Equation (4.4) is implemented by the multiplication of the nth chip by the complex conjugate of the (n-1)th chip. Then the signal is multiplied by the PN sequence (equation (4.5)) and passed through a correlator before being demodulated to recover the information.

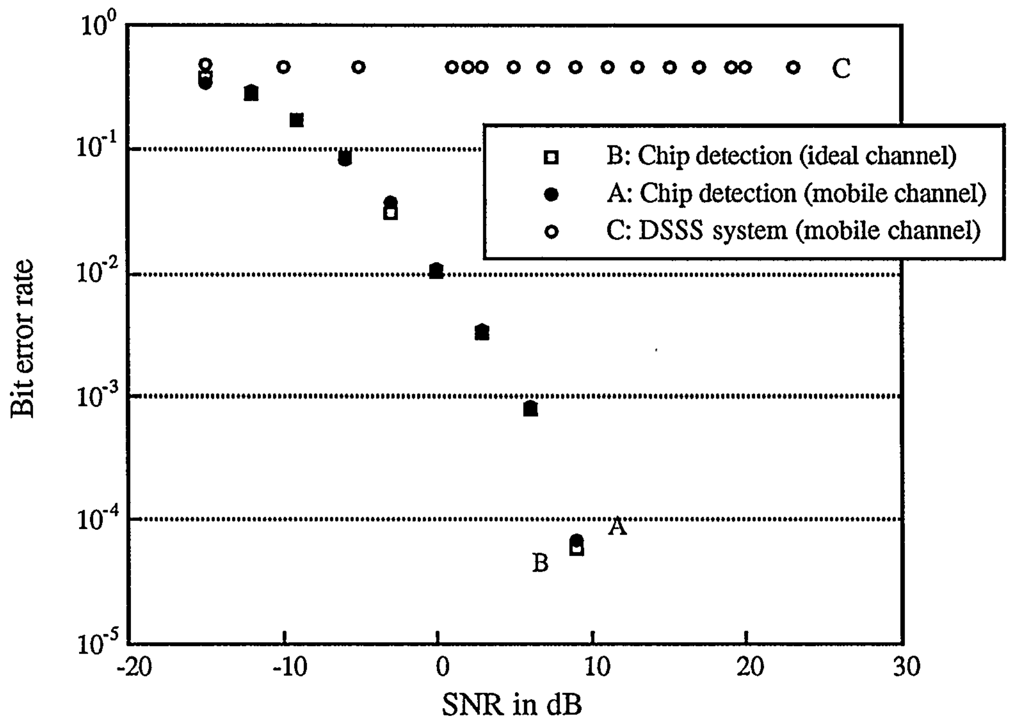

Figure 4.3 BER curves for the chip detection method and the DSSS communication system for PG=127.

4.4 Performance of the chip detection method

The performance of the system is evaluated for all the processing gains investigated in this study (15, 31, 63 and 127) for a fixed vehicle velocity of 100km/h.

Figure (4.3) shows three BER curves corresponding to the communication system in figure (4.2) for a PG = 127. The irreducible BER of curve C in figure (4.3) is eliminated by the chip detection communication system as shown in curve A. The same system performance with an ideal channel is also shown as curve B in figure (4.3). The chip detection system with a mobile channel with phase distortion performs as well as the chip detection system when the channel is ideal i.e. no phase distortion.

However, some SNR loss has to be tolerated with chip detection (figure (4.4)). Curve B of figure (4.4) is the same curve B shown in figure (4.3). Curve A of figure (4.4) is obtained by a conventional DSSS communication system with no chip detection when the channel is ideal i.e. with no phase distortion. At a BER of 10^{-4} the ideal channel performance for the chip detection method is about 5-6dB poorer than the DSSS communication system when the channel is ideal.

Figure (4.5) shows three BER curves corresponding to a PG = 63. Here too the chip detection method is able to eliminate the error floor (curve C in figure (4.5)) and its performance shown in curve A is as good as when chip detection is applied over an ideal channel (curve B).

Figure (4.6) shows the SNR loss corresponding to chip detection with respect to a conventional DSSS system with no chip detection. At a BER of 10^{-4} the SNR loss is about 5dB.

Figure (4.7) shows the performance of the chip detection system for PG=31. The error floor in curve C is eliminated by this system as shown in curve A. However, the SNR loss for this method at a BER of 10^{-4} is about 3.5 dB as shown in figure (4.8).

Finally, figure (4.9) shows the performance of the chip detection system for PG = 15. Once again the irreducible BER floor (curve C in figure (4.9)) is eliminated (curve A) by this system at the lowest processing gain investigated in this study.

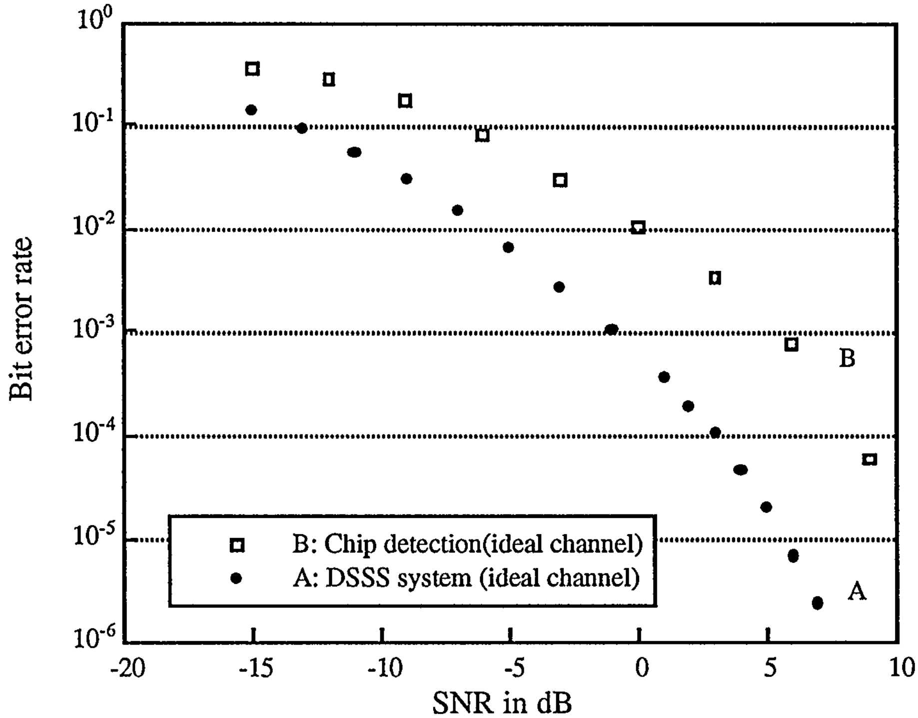

Figure 4.4 SNR loss of the chip detection method illustrated for PG=127.

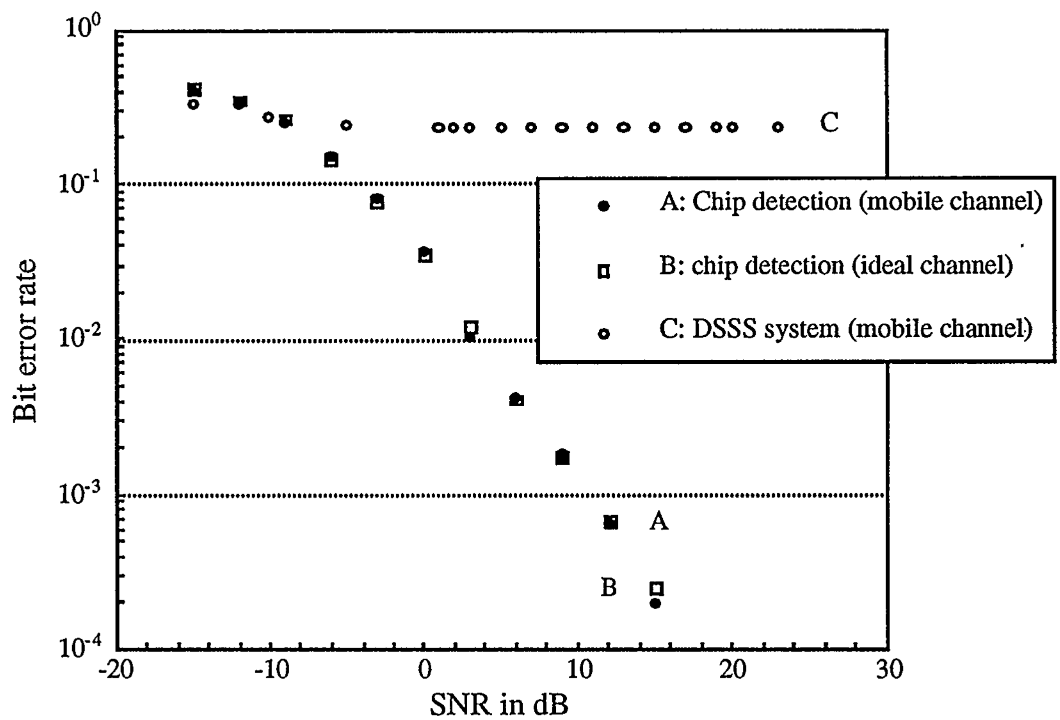

Figure 4.5 BER curves for the chip detection method and the DSSS communication system for PG=63.

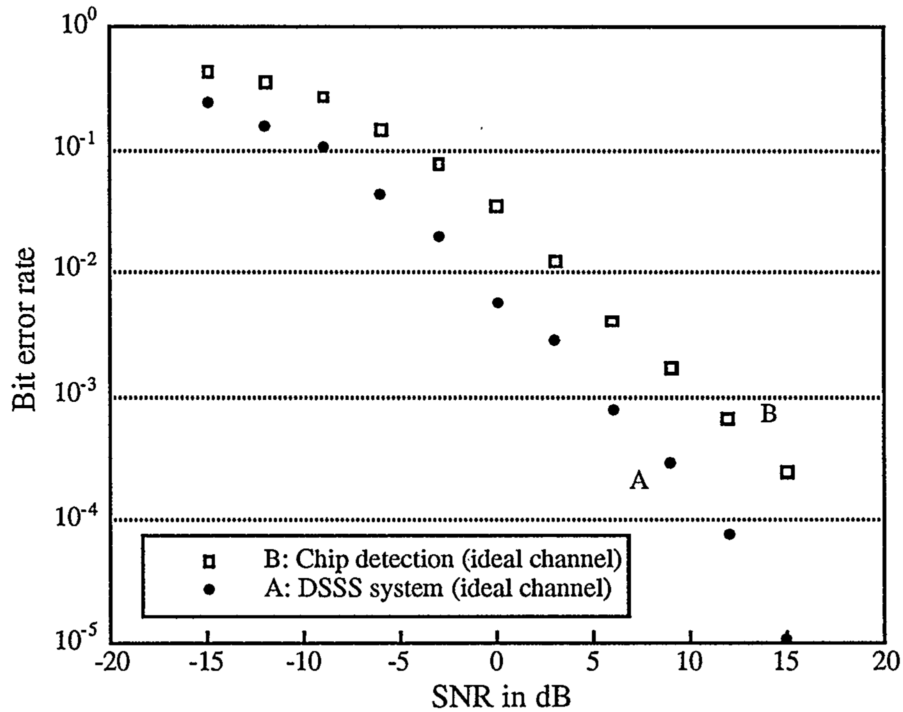

Figure 4.6 SNR loss of the chip detection method illustrated for PG=63.

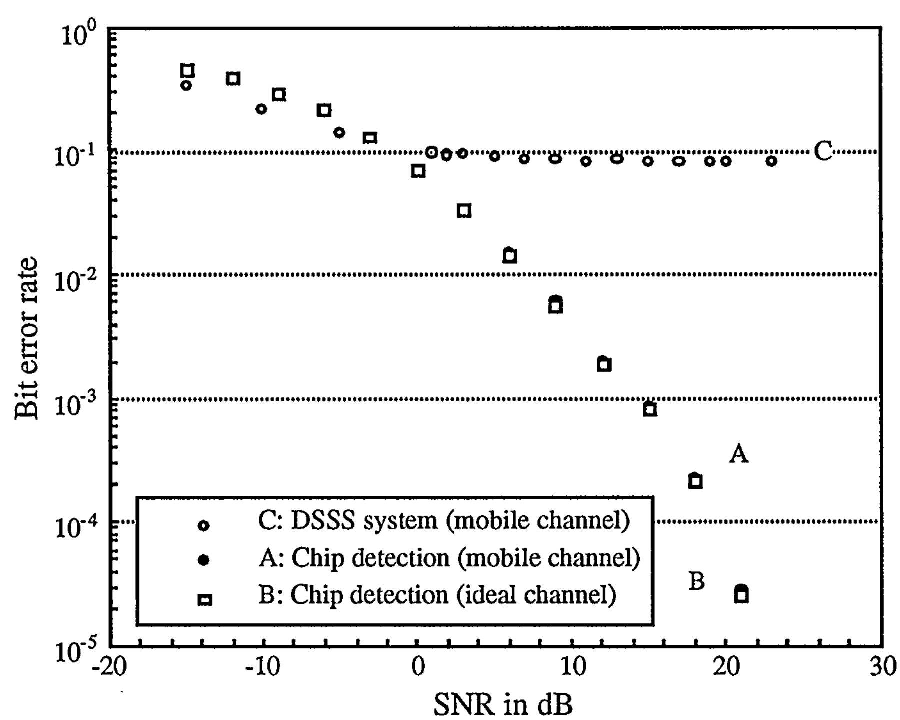

Figure 4.7 BER curves for the chip detection method and the DSSS communication system for PG=31.

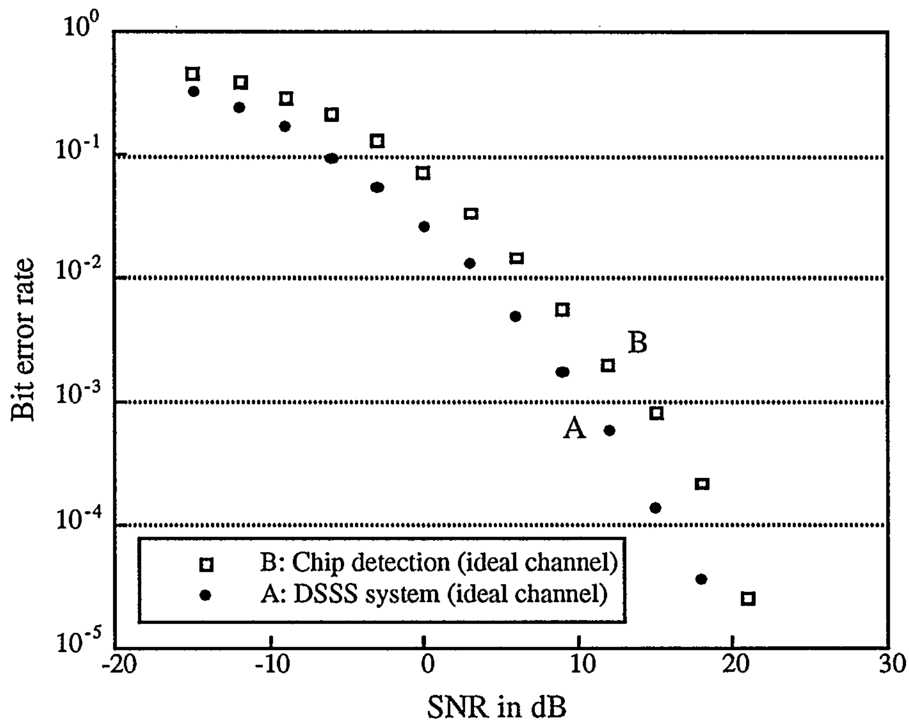

Figure 4.8 SNR loss of the chip detection method illustrated for PG=31

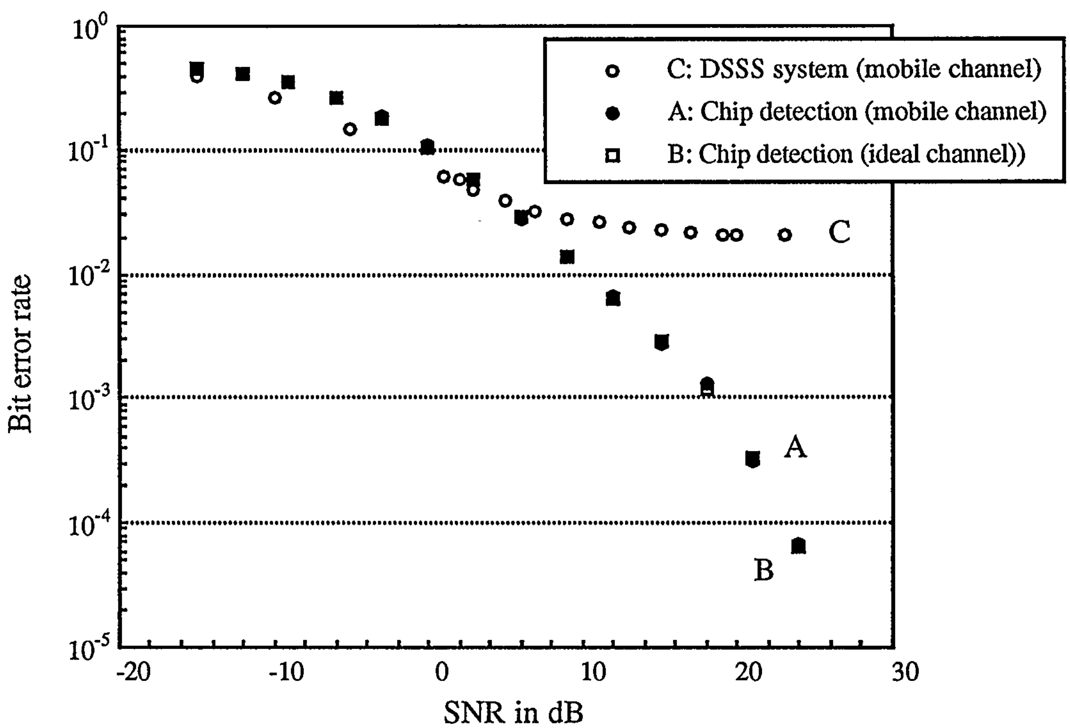

Figure 4.9 BER curves for the chip detection method and the DSSS communication system for PG=15.

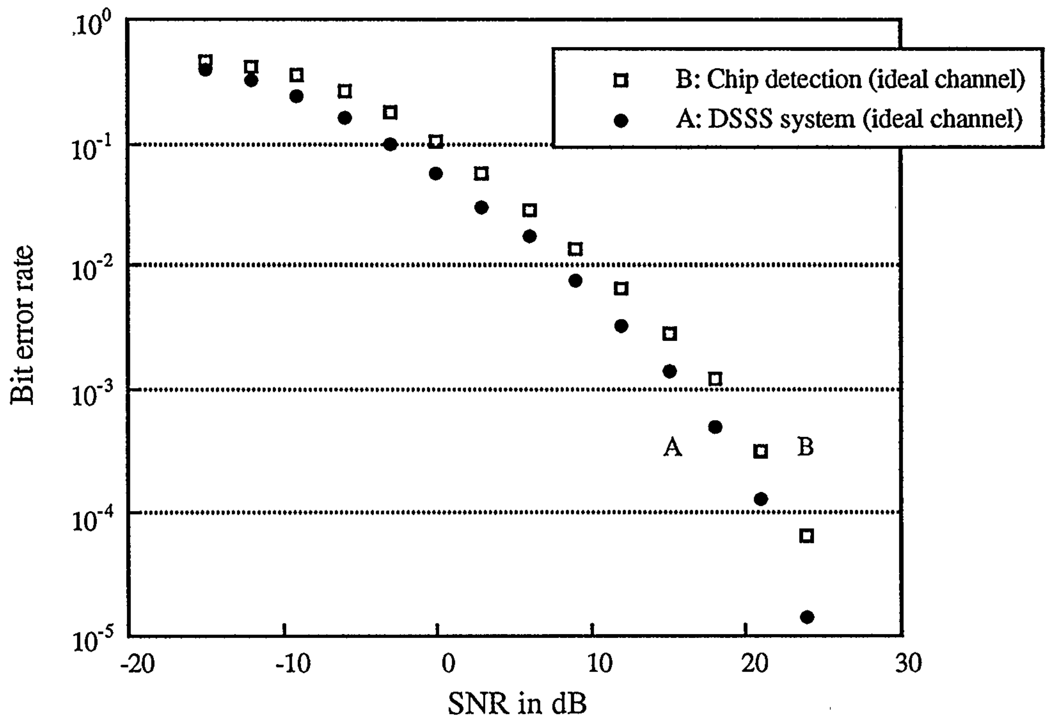

Figure 4.10 SNR loss of the chip detection method illustrated for PG=15.

According to figure(4.10) the SNR loss associated with this method is now at its lowest (i.e. 2dB) at a BER of 10^{-4} with respect to the DSSS system with an ideal channel.

4.5 Concluding Remarks

In this chapter, we have introduced a novel demodulation technique which eliminates the effect of the phase distortion due to flat fast fading on a DSSS/DQPSK system. Such a technique eliminates the error floor caused by the phase distortion at the expense of some SNR loss.

In the next chapter, Binary FSK is considered together with DSSS using a differential receiver similar in concept to Chip detection.

Chapter five

Binary FSK system and differential detection

5.1 Why Binary FSK?

Both chapters two and three focused on a DSSS communication system that is based on DQPSK modulation. In each chapter, a technique was discussed in an attempt to eliminate the BER floor caused by the phase distortion due to flat fast fading. This chapter analyzes a third technique together with Binary Frequency Shift Keying (Binary FSK) spread using DSSS.

If average error rate due to envelope fading alone is considered, Binary FSK would perform as well as Differential Phase Shift Keying (DPSK) [11]. However, in a random FM environment Binary FSK outperforms DPSK. The irreducible BER, P_{BFSK}, for BFSK is related to the irreducible BER, P_{DPSK}, for DPSK as follows:

$$P_{BFSK} = \frac{1}{4\pi^2}\left(\frac{f_s}{f_{dev}}\right)^2 P_{DPSK} \tag{5.1}$$

where f_s is the signal bandwidth and f_{dev} is the frequency deviation for BFSK. For a typical frequency deviation, i.e. $\frac{f_s}{2} = f_{dev}$, the P_{BFSK} is 10 times smaller than P_{DPSK}. Mobile channels in an urban environment suffer from envelope fading as well as from the random FM phenomena. Therefore Binary FSK should perform at least as well as DPSK, if not better. Chapters two and three studied

DQPSK communication systems. DQPSK signal constellations are spaced every 90 degrees while DPSK signal constellations are spaced every 180 degrees (table 5.1).

DQPSK Symbol	Phase change
00	0^{o}
01	90^{o}
11	180^{o}
10	270^{o}

DPSK Symbol	Phase change
1	0^{o}
0	180^{o}

Table 5.1 DPSK and DQPSK symbols with differential phase.

Simulations have shown that DQPSK has an irreducible bit error rate of 10^{-3} in flat fast fading channels. The Irreducible bit error rate for DPSK can be calculated using the following equation [14]:

$$P_{DPSK} = 0.5\left(\frac{\pi f_m}{f_s}\right)^2 \tag{5.2}$$

where f_m is the maximum doppler spread and f_s is the signal bandwidth. For a signal bandwidth of 24kHz and a maximum doppler spread $f_m = f_d = 77.78Hz$, P_{DPSK} will be $5.18{*}10^{-5}$. This was also tested by simulations and found to be true.

Hence DPSK is much more immune to phase noise and other effects than DQPSK. By the same token, BFSK should also be more immune to phase noise and other distortions than DQPSK. This is particularly true for BFSK with differential detection since it gives better performance in channels with severe delay distortion [1]. Incoherent receivers for BFSK such as differential detection can be implemented with ease [13], [21]. In general, all FSK modulation schemes are immune to certain non-linearities because they are constant envelope based [13].

5.2 Binary FSK modulation

A Binary FSK signal $S(t)$ can be expressed mathematically as:

$$S(t) = A\cos\left(2\pi\, f_c t + \theta(t)\right) \tag{5.3}$$

where f_c is the carrier frequency and $\theta(t)$ is the phase. It is a nonlinear modulation scheme with a constant envelope where the information is conveyed by varying the carrier frequency in response to the information data stream [8]. If a zero is transmitted we have

$$\theta(t) = -2\pi\, f_{dev} t + \phi_0$$

and if a one is transmitted we have

$$\theta(t) = 2\pi\, f_{dev} t + \phi_1$$

where f_{dev} is the frequency deviation. ϕ_0 and ϕ_1 are the initial phase angles of the two oscillators. Without loss of generality, let us assume that ϕ_0 and ϕ_1 are zero. Hence no phase continuity is assumed. Thus, the signal is given by

$$S_1(t) = A\cos\left(2\pi\left(fc - f_{dev}\right)t\right) \tag{5.4}$$

if a zero is transmitted, else it is given by

$$S_2(t) = A\cos\left(2\pi\left(fc + f_{dev}\right)t\right) \tag{5.5}$$

$S_1(t)$ and $S_2(t)$ in equations (5.4) and (5.5) can be generated either by two independent oscillators with no phase continuity or by applying the information signal to a VCO (voltage controlled oscillator) with phase continuity.

Signals $S_1(t)$ and $S_2(t)$ are called space and mark respectively and they are approximately orthogonal if $2f_{dev}T$ is an integer. Improved uncorrelatedness (orthogonality) can also be obtained when $f_{dev}T >> 1$ [12]. Hence, a higher modulation index h will give less correlation between $S_1(t)$ and $S_2(t)$.

The modulation index h is defined as follows [12]:

$$h = 2f_{dev}T \tag{5.6}$$

where T is the symbol duration.

5.3 Differential detection of Binary FSK

Differential detection of Binary FSK signals was first analyzed by Anderson et al [1]. They showed that differential detection is superior in performance to frequency discrimination or zero-crossing counter in channels with severe delay distortion.

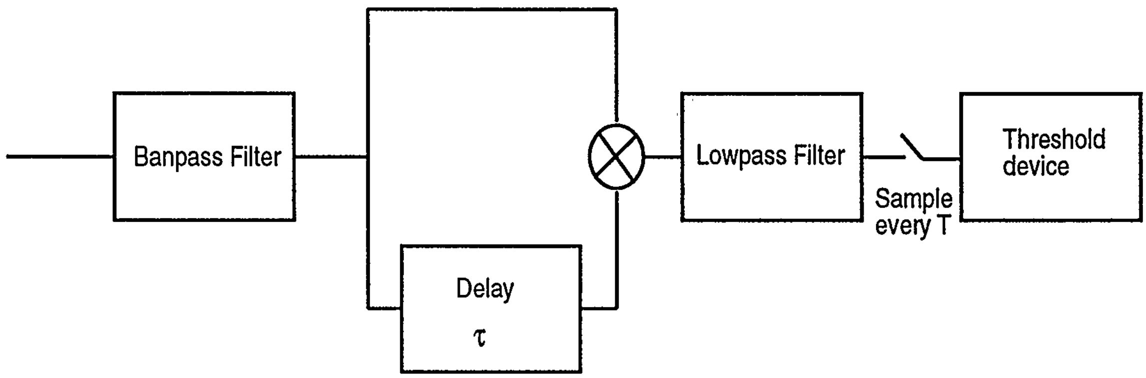

Figure 5.1 Differential detector for Binary FSK.

Figure (5.1) shows a differential detector for Binary FSK [4]. The receiving bandpass filter shown in figure (5.1) performs two contradictory tasks [2]:

1) To minimize the out-of -band noise and interference from the detector input (i.e. it has to be narrow band).

2) To pass the in-band signal with the minimum possible distortion (i.e. it has to be wide band).

The signal at the output of the received bandpass filter is given by the following equation [4]:

$$y_1(t) = A\cos(\omega_c t + \phi(t)) + n_1(t)\cos(\omega_c t) - n_2(t)\sin(\omega_c t) \tag{5.7}$$

where $\phi(t) = \dfrac{\pi\, h a_n t}{T} + x_n$ (5.7')

$\phi(t)$ is the data dependent instantaneous phase in the interval $nT \le t \le (n+1)T$. ω_c is the IF frequency where all the processing takes place. The variable h is the modulation index and T is the symbol duration. The variable a_n can take the values: 1 or -1 with equal probability. Variables $n_1(t)$ and $n_2(t)$ are narrow band

Gaussian noise variables. In equation (5.7'), if phase continuity is not required from one symbol to the other, x_n can be omitted. The differential detector employs an arbitrary delay τ, where $y_1(t)$ is multiplied by the delayed version $y_1(t-\tau)=y_2(t)$. Then $y_2(t)$ can be written as:

$$\begin{aligned} y_2(t) &= A\cos(\omega_c t-\omega_c\tau+\phi(t-\tau))+n_1(t-\tau)\cos(\omega_c t-\omega_c\tau) \\ &\quad -n_2(t-\tau)\sin(\omega_c t-\omega_c\tau) \end{aligned} \tag{5.8}$$

Usually, $y_1(t)$ is delayed in such a way that $\omega_c\tau=\frac{\pi}{2}$. Then equation(5.8) can be simplified to equation (5.9):

$$y_2(t)=A\sin(\omega_c t+\phi(t-\tau))+n_3(t)\sin(\omega_c t)+n_4(t)\cos(\omega_c t) \tag{5.9}$$

where $n_3(t)=n_1(t-\tau)$ and $n_4(t)=n_2(t-\tau)$. The lowpass filter output is obtained by multiplying $y_2(t)$ by $y_1(t)$ and omitting the "$2\omega_c$" components from the product, since the lowpass filter is designed to eliminate all high frequency components and to further reduce the noise in the signal. The output of the lowpass filter is denoted by $Z(\tau)$ where

$$\begin{aligned} 2Z(\tau) &= [A\cos\phi(t)+n_1][A\sin\phi(t-\tau)+n_4] \\ &\quad -[A\sin\phi(t)+n_2][A\cos\phi(t-\tau)+n_3] \end{aligned} \tag{5.10}$$

For the noise free case equation (5.10) can be simplified to equation (5.11):

$$2Z(\tau)=-a_n A^2\sin\left(\frac{\pi h\tau}{T}\right) \tag{5.11}$$

since $\phi(t)-\phi(t-\tau)=\dfrac{\pi h a_n\tau}{T}$

If $\frac{\pi h \tau}{T} << \frac{\pi}{2}$, τ can be increased to maximize the distance between the two possible values that $Z(\tau)$ can take, when a_n is 1 or -1. Hence, a simple threshold device after the lowpass filter is sufficient to recover the information.

5.4 Binary FSK system without the receive bandpass filter

Figure (5.2) shows a Binary FSK communication system which also employs DSSS techniques. This system is different from other communication systems discussed in chapters two and three because it uses Binary FSK as the modulation scheme. Note that the receiver in figure (5.2) employs a differential detector. Although a typical differential detector has a bandpass filter at the receiver input, it is omitted in this communication system. Later on, the receive bandpass filter will be re-instated at the receiver input. Then both systems will be compared with respect to the effectiveness of the receive bandpass filter.

Information is generated at a rate of 90.71 bits per second. It is then modulated using Binary FSK with modulation indices of h = 1, 2, 4, and 10 before being spread with a PN sequence of length 254. The chip rate is fixed at 23.041kHz. Hence, the chip duration is 43.4 micro seconds. The total bandwidth occupied by the signal after the spreading is approximately given by [17]:

$$BW = 2(W + fd) \tag{5.12}$$

where $W = \frac{23.041 * 10^{+3}}{2}$.

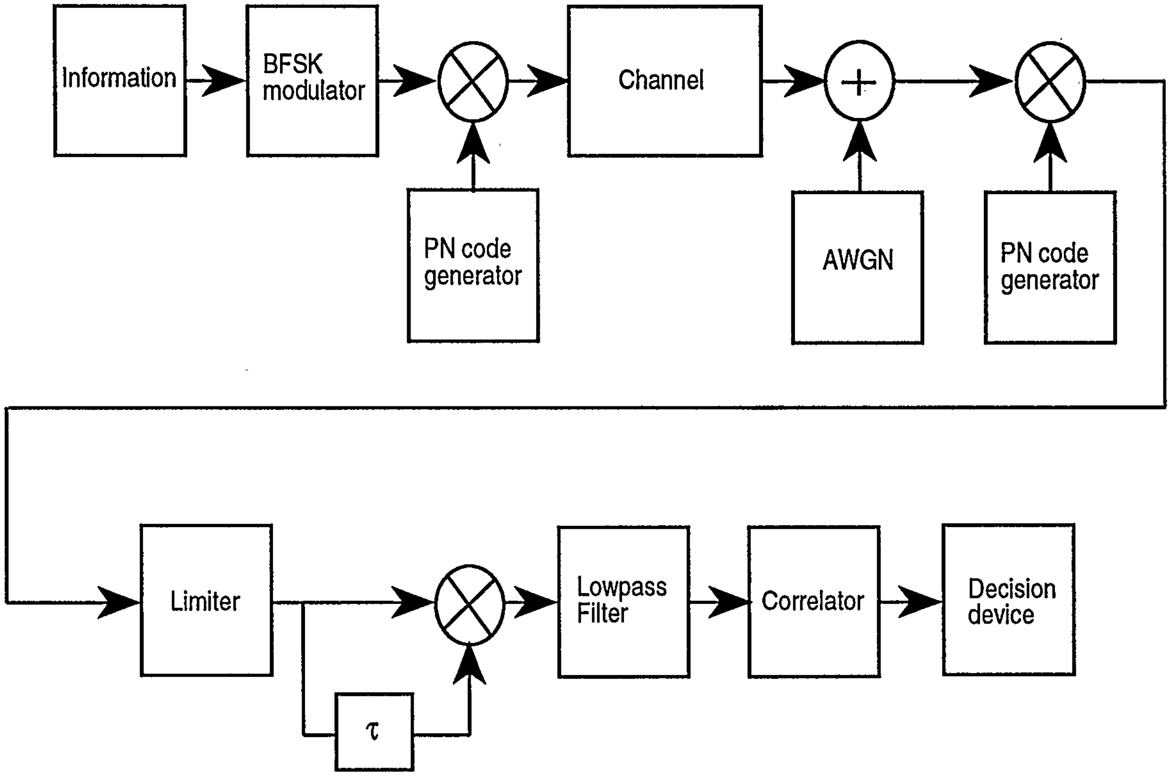

Figure 5.2 Binary FSK communication system without the receive bandpass filter

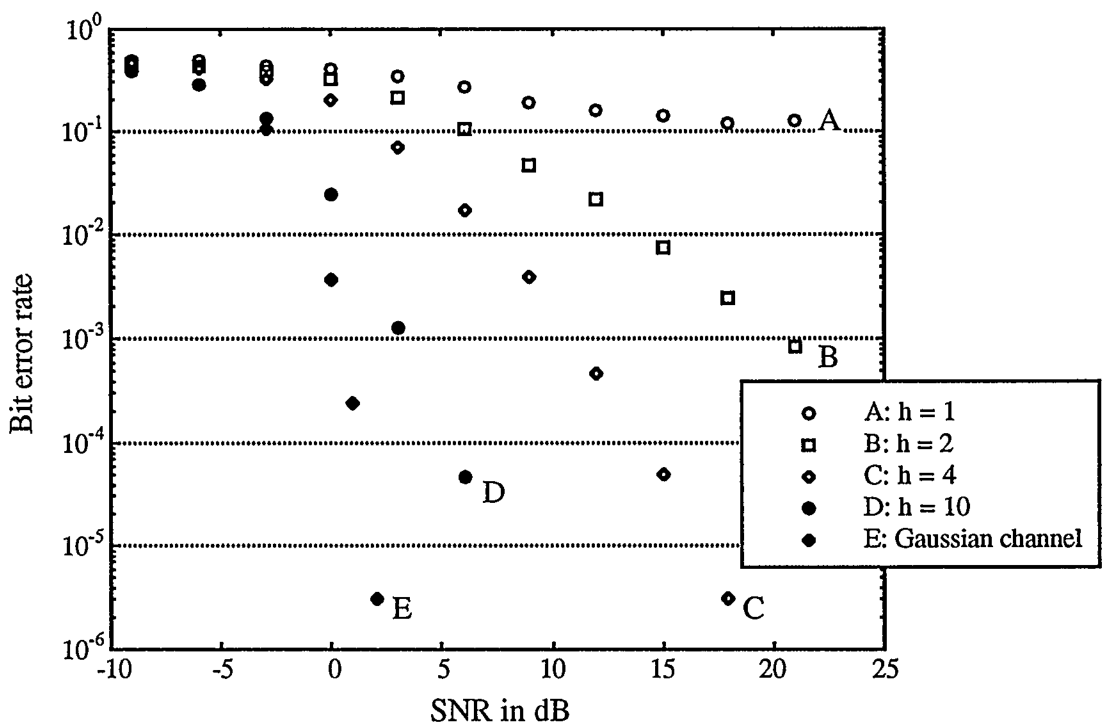

Figure 5.3 Performance of the communication system shown in figure 5.2 for different modulation indices and for a Gaussian channel.

The maximum bandwidth occurs when $h = 10$ or $f_{dev} = 453.6\text{Hz}$, and it is 23.948kHz.

The performance of the communication system in figure 5.2 is illustrated in figure (5.3) for $h =$ 1, 2, 4, and 10 for both a Gaussian and a mobile flat fast fading channel. Curve E in figure 5.3 shows the performance of this system in a Gaussian noise channel with $h = 10$. Over a mobile flat fast fading channel, BFSK with $h =$ 1 does not succeed in eliminating the BER floor as shown in curve A in figure (5.3). Due to improved orthogonality between signals $S_1(t)$ and $S_2(t)$ [12] the communication system shown in figure 5.2 performs well at higher modulation indices such as 2, 4, and 10 (curves B, C, D of figure 5.3). Another reason for this improved performance is seen in equation 5.11 where $|Z(\tau)|$ is larger when h is larger. Hence the two possible values that $Z(\tau)$ can take will be at a distance further apart from each other.

In figure (5.4) the communication system has a bandpass filter at the receiver input. Since the computer simulations are performed for lowpass equivalent signals the bandpass filter becomes a lowpass filter for simulation purposes only. The lowpass filter is designed for the following cut off and stop band frequencies for a maximum modulation index of $h = 4$:

Cut off frequency = 300Hz

Stop band frequency = 417Hz

Pass band to stop band attenuation = 17.91dB or 7.857 times

Simulations at $h = 10$ were not performed to save simulation time as the bit error rates are very low. An FIR filter with 101 taps was used in the simulations. However, in practice a 7th order Butterworth filter is sufficient.

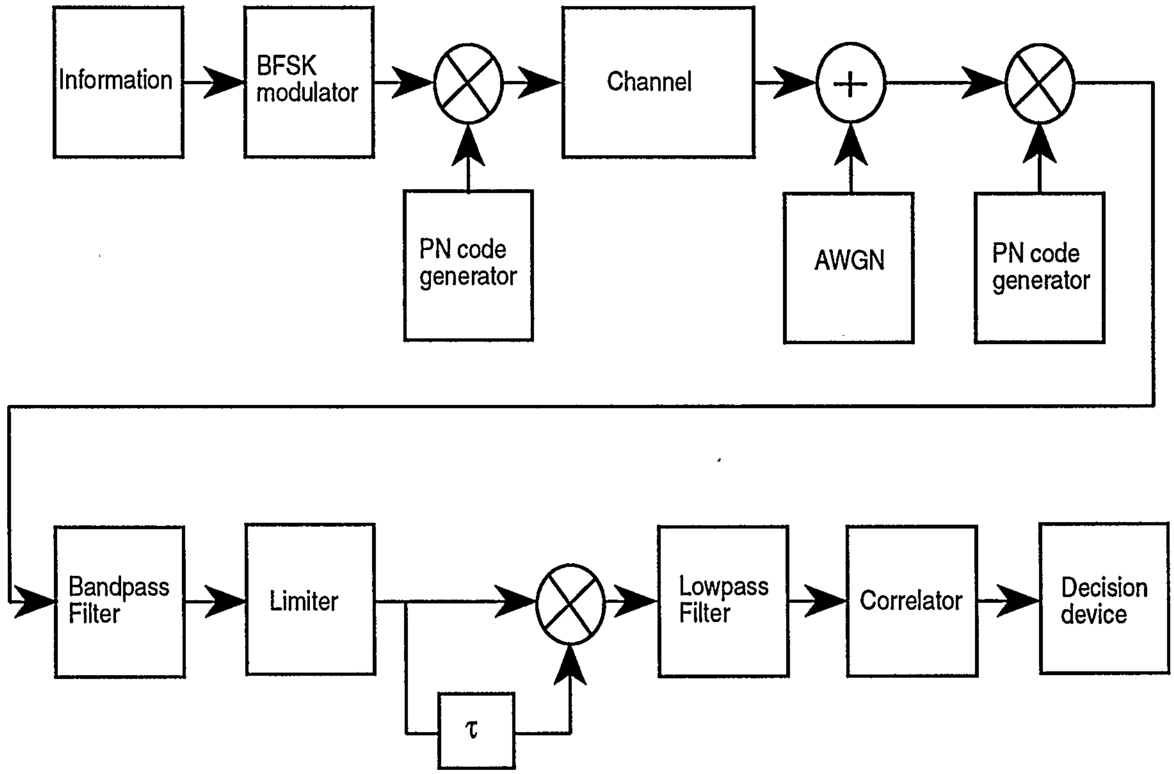

Figure 5.4 Binary FSK communication system with the receive bandpass filter

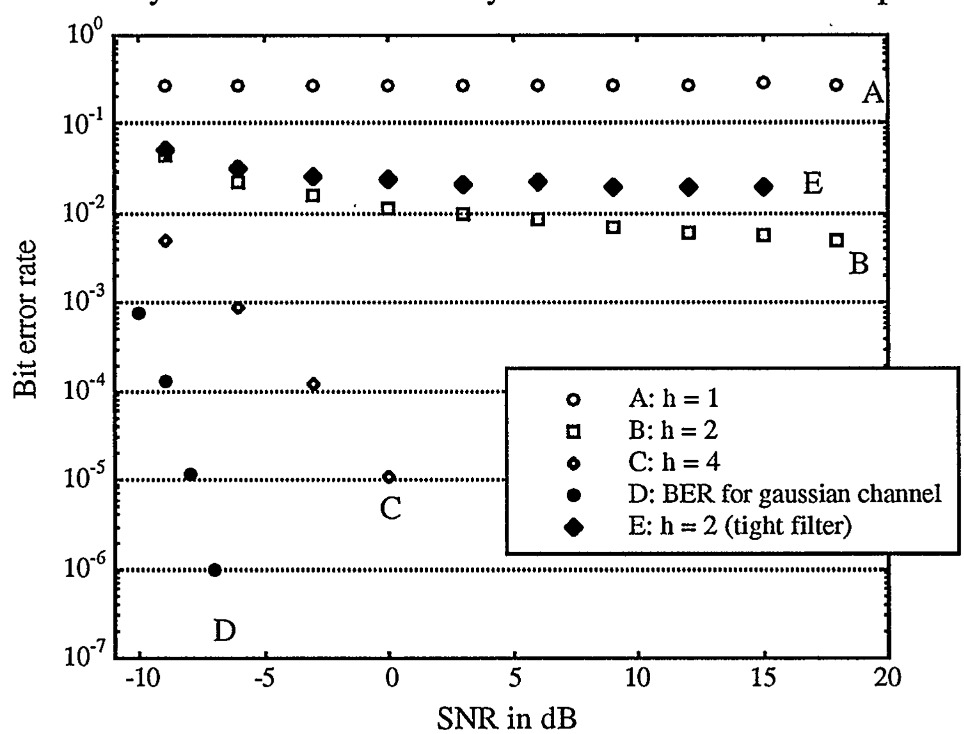

Figure 5.5 Performance of the communication system shown in figure 5.4 for different modulation indices and for a Gaussian channel.

Figure 5.5 shows the simulation results obtained for the communication system in figure 5.4. Three BER curves are obtained for $h = 1, 2,$ and 4. Unlike curve B in figure 5.3 ($h = 2$), curve B of figure 5.5 ($h = 2$) experiences a bit error floor at high SNRs. This is mainly due to the inter symbol interference (ISI) of the receive bandpass filter and the phase distortion (random FM) of the mobile channel. BER curves A, B, C, and D were simulated with a fixed receive bandpass filter with a cut off frequency of 300Hz. Curve E in figure (5.5) corresponds to curve B with a tight filter of 200Hz cut off frequency. Since the BER with a tight filter (curve E in figure (5.5)) is worse compared with the loose filter (curve B in figure (5.5)), it can be concluded that ISI is more significant at $h = 2$ than the rejected in band noise. The system performed well for a modulation index of $h = 4$ and eliminated the BER floor completely. A BER of 10^{-5} was obtained at a SNR of 0dB. Curve D shows the performance of the system for a Gaussian channel at $h = 4$.

More simulations were performed to investigate the effect of ISI and the in-band noise towards the system performance without random FM. In this case, a filter with a smaller cut off frequency is used for lower in band noise and higher ISI. Curve C in figure (5.6) is obtained with $h = 4$ and curves A and B are obtained with $h = 2$. Since curve C is obtained with a receive bandpass filter with a cut off frequency of 300Hz, it contains more in-band noise and less ISI compared with curve B. However, curve B has more ISI and less in-band noise compared with curve A. Both curves A and C contain the same amount of ISI and in-band noise, however, a high modulation index ($h = 4$) with curve C improves the BER over curve A.

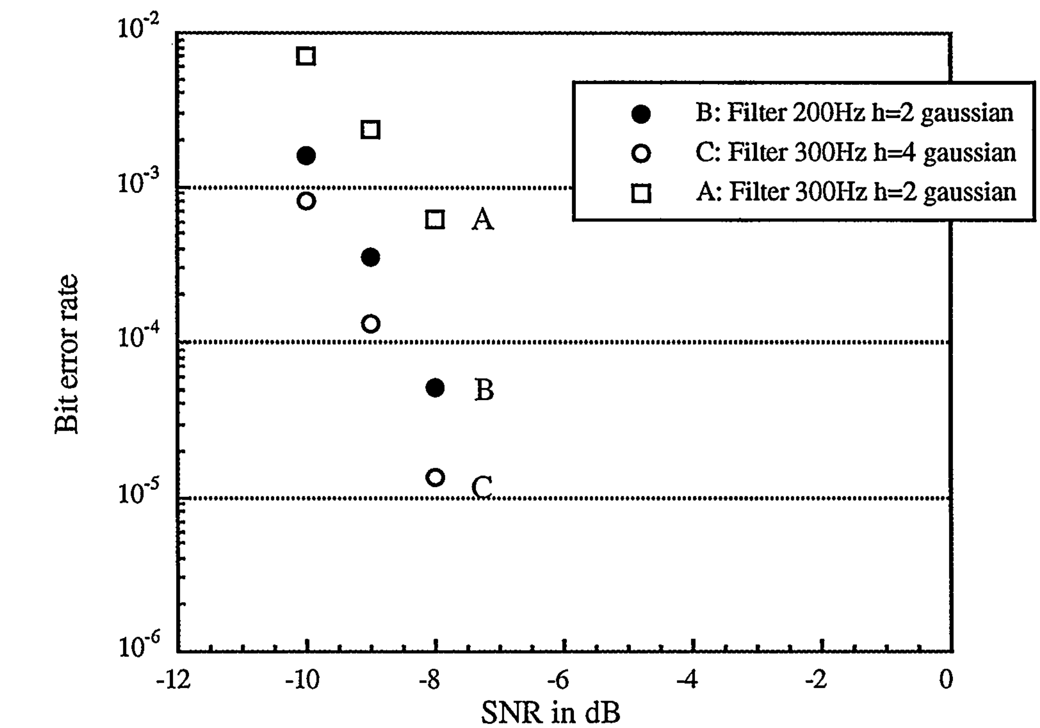

Figure 5.6 Comparison of ISI and in-band noise without random FM.

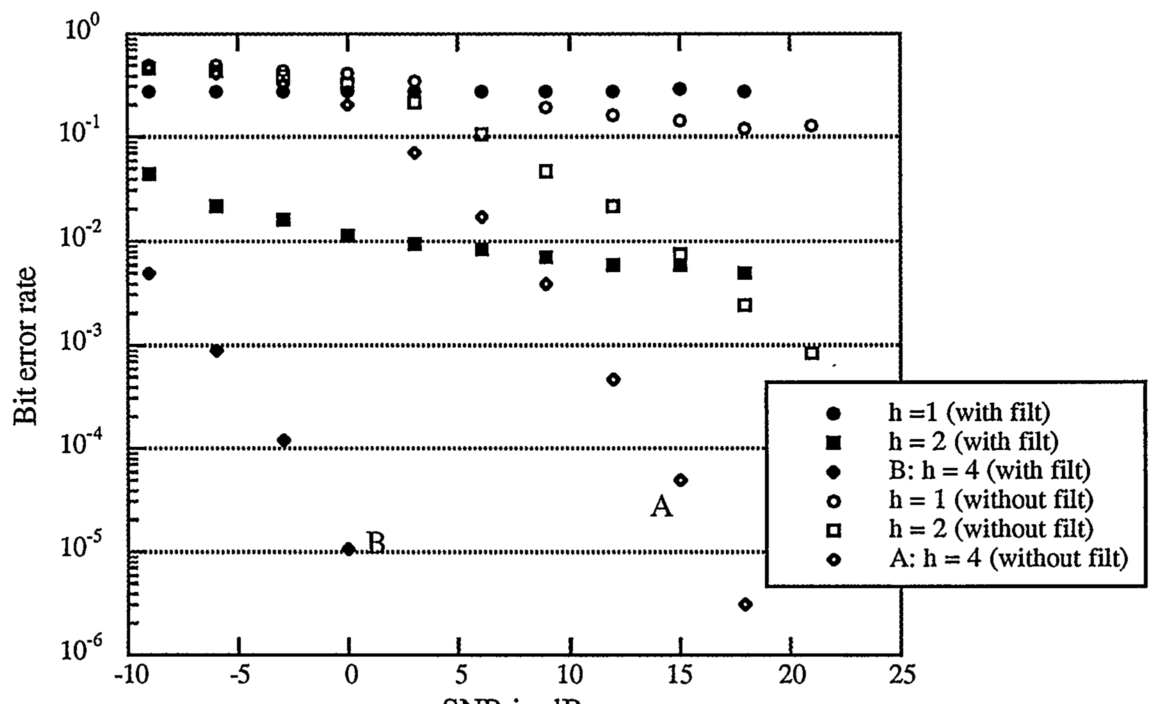

Figure 5.7 Performance of the Binary FSK communication systems with and without the receive bandpass filter for different modulation indices.

Figure (5.7) shows the BER curves for $h = 1$, 2, and 4 for a communication system with and without the receive bandpass filter. For $h = 4$ the communication system without the receive bandpass filter achieves a BER of 10^{-5} at an SNR equal to 17dB. Hence at a BER of 10^{-5} the communication system with the receive bandpass filter has a 17dB advantage over the other communication system.

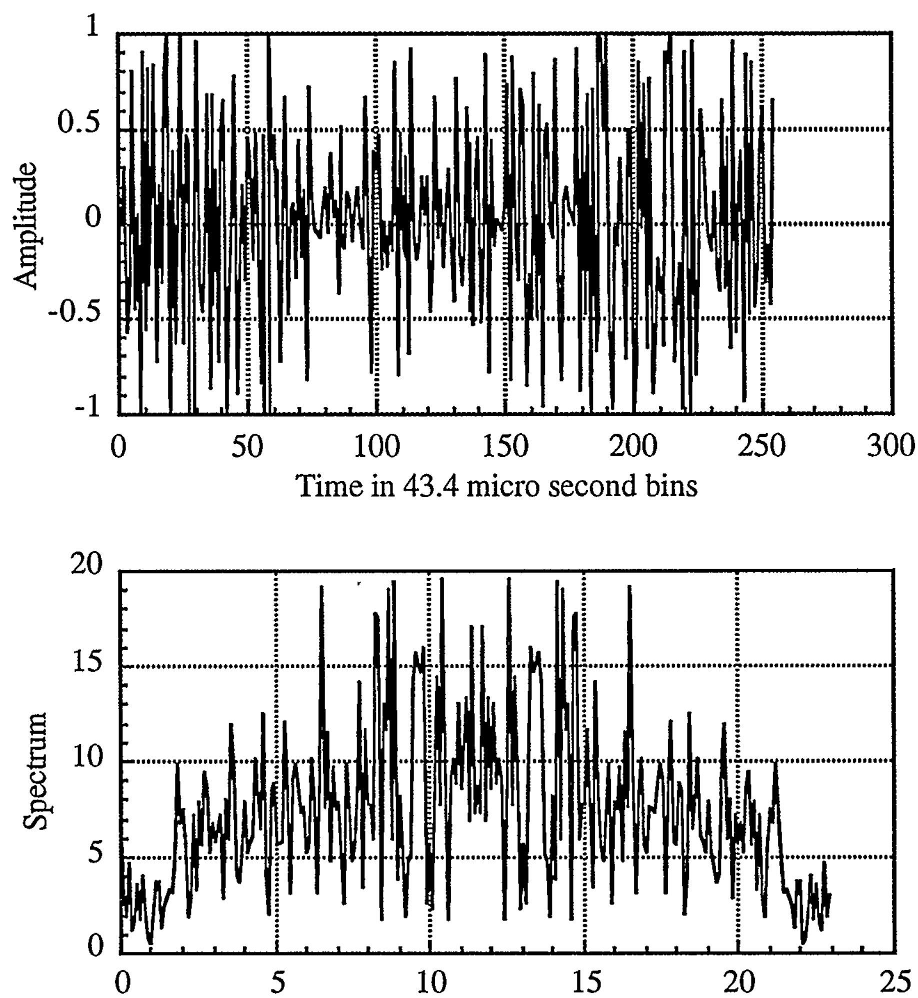

Figure 5.8 Signal and the Spectrum of the Binary FSK communication system without the receive bandpass filter.

A Binary FSK signal is illustrated in figures 5.8 and 5.9 corresponding to a long train of information symbols "1". Figure(5.8) corresponds to the system in figure

(5.2) while 5.9 corresponds to the one in 5.4. The same amount of noise is added in both cases so that the signal to noise ratio is 5dB at the input of the receiver.

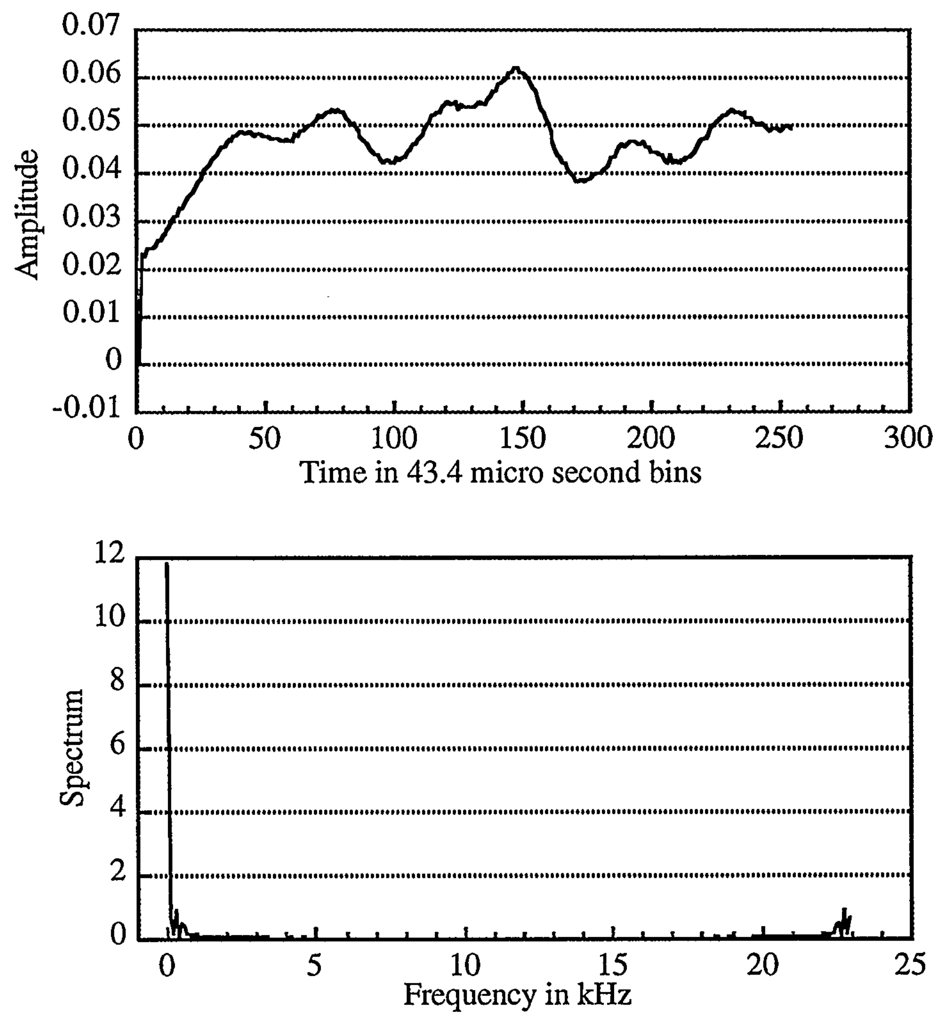

Figure 5.9 Signal and the Spectrum of the Binary FSK communication system with the receive bandpass filter.

Figures 5.8 and 5.9 show both the signal and its Fast Fourier Transform (FFT) just after the lowpass filter. If out-of-band noise is not filtered by the bandpass filter (figure 5.8), the differential detector amplifies noise. Hence, the signal is buried in noise. The spectrum shown in figure 5.8 is also noise like. However, the information signal can be recovered when the out-of-band noise is eliminated by the receive bandpass filter (figure 5.9). The signal in figure 5.9 shows some distortion due to channel fades and in-band noise. However, this noise amplification phenomenon is not analyzed due to the non-linear behaviour of the Binary FSK communication system.

5.5 Concluding Remarks

In this chapter, the effect of the BPF on the performance of a BFSK/DSSS system was analyzed when differential detection is employed at the receiver. It was found that for a higher modulation index such as $h=4$ the performance of the BFSK system is 17dB better with the BPF than without. However, the system with the BPF does not perform as well at $h=2$ due to increased distortion from ISI. Generally, increasing h improves the BFSK/DSSS system performance in a fast fading environment in spite of the increased in-band noise. A simple simulation was performed in order to compare BFSK/DSSS and DQPSK/DSSS communication systems. A modulation index of $h = 4$ was used while the processing gain was fixed at PG = 254. It was found that the BFSK/DSSS communication system with the bandpass filter has a 9dB advantage over the DQPSK/DSSS communication system at a bit BER of 10^{-4}.

Chapter six

Conclusion

This thesis has investigated three detection techniques to receive a narrowband DSSS signal over mobile flat fast fading channels when vehicles move at high speeds such as 100km/h. Conventional solutions such as diversity, pilot tone, pilot symbol, or coding and interleaving fail to eliminate the BER floors in this case. Such an environment is similar to the one that exists in wide area paging where narrowband (25kHz) data are transmitted from people on the move on the reverse link of a two-way paging system.

The first two techniques are based on DQPSK/DSSS with phase correction. The last technique uses Binary FSK/DSSS without explicit phase correction. DSSS is used in all the techniques discussed in this thesis since it can help overcome the flat fading nature of the narrowband channel when the channel is mobile and hence can help preserve transmitter power at the pager.

The first technique is based on the Hilbert transform where it is used to estimate the differential phase of the received signal. Hence large phase distortions due to fades can be eliminated with this technique. When the vehicle moves at 100km/h, this Hilbert transform based communication system eliminates the BER floor at lower processing gains such as 15 or lower. However, this method fails to eliminate BER floor at higher processing gains such as 31, 63, and 127 as a result of an accumulation of small phase offsets caused by doppler. The phase correction algorithm used by this technique is unable to eliminate such an accumulation. With added processing to an already complex receiver, this algorithm can be modified to eliminate such small offsets. This can be achieved by multiplying the small phase offsets by a larger value and the large phase distortions by a smaller value. Once the sign ambiguity of the Hilbert transform estimate is taken care of, the error between the differential phase estimate and the received differential phase can be minimized so that we are able to eliminate the error floor at high processing gains.

Chapter four introduces a novel demodulation technique called Chip detection which eliminates the small phase offsets caused by doppler. This is achieved by multiplying each chip by the complex conjugate of the previous chip. Hence the name “Chip detection” which eliminates the error floor at all the processing gains such as 15, 31, 63 and 127 at the expense of some SNR loss. At a BER of 10^{-4} this SNR loss can be 5-6 dB for a processing gain of 127 when compared with the conventional DSSS communication system with an ideal channel. However, this SNR loss is small with low processing gains. For example, at a processing gain of 15 this loss is about 2 dB. Another drawback with this technique is the need to transmit an extra reference chip with each symbol. However, this overhead is small at high processing gains.

The final technique which is based on Binary FSK/DSSS is discussed in chapter five. Binary FSK is robust and works well in random FM environments. A Differential detector is used to demodulate the Binary FSK signal. Differential detection is an incoherent demodulation technique. Hence, it is easy to implement and inexpensive. Performance of this BFSK/DSSS communication system is investigated only at a processing gain of 254 with and without the receive bandpass filter for h = 1, 2 and 4. BFSK communication system with the receive bandpass filter achieved a BER of 10^{-5} at a SNR of 0 dB whereas the BFSK communication system without the receive bandpass filter achieved the same BER at 17 dB SNR. A modulation index of $h = 4$ was used in both cases. The function of the receive bandpass filter is to eliminate out-of-band noise prior to the detection since the differential detector amplifies all out-of-band noise. Hence, the BFSK system with the receive bandpass filter has a 17dB advantage at a BER of 10^{-5} over the BFSK system without the filter.

A simple simulation was performed to compare the performance of the DQPSK/DSSS system with chip detection to the BFSK/DSSS communication system with a receive bandpass filter. A modulation index of $h = 4$ is assumed for BFSK and a PG = 254 was used in both cases. A BER of 10^{-4} was achieved with the BFSK system with a SNR of only -3 dB, while the DQPSK system achieved it with 6dB. Hence the BFSK system has a 9dB advantage over the DQPSK system at a PG = 254 except that the latter has double the throughput than the former.

Although a complete analysis of the BFSK system was not performed in this thesis, it is recommended that this type of communication system be used at all processing gains when wireless data are transmitted from a mobile moving at high speeds in an urban environment.

References

[1] Anderson, R. R., Bennett, W. R., Davey, J. R., and Salz, J., " Differential Detection of Binary FM", The Bell system technical journal, vol. 44., pp. 111-159, 1965.

[2] Bennett, W. R., and Salz, J., "Binary Data Transmission by FM over a Real Channel", The Bell system technical journal, Vol. 42., pp. 2387-2426, September 1963.

[3] Cox, C. D., "Wireless Personal Communications: What is it?", IEEE Personal Communications, pp. 20-35, April 1995.

[4] Ekanayake, N., "On Differential Detection of Binary FM", IEEE Transactions on communications", Vol. COM-32, No. 4, pp. 469-470, April 1984.

[5] Fattouche, M., and Zaghloul, H., "Estimation of phase differential of signals transmitted over fading channels", Electronics Letters, Vol. 27 No. 20, pp. 1823-1824, September 1991.

[6] Fattouche, M., Olasz, E. B., Scott, K. E., and Zaghloul, H., " Modified simulation of the urban radio propagation radio channel", Electronics Letters, Vol. 29, pp. 1825-1826, October 1993.

[7] Fattouche, M., and Zaghloul, H., "Data Communications over the Mobile Radio Channel using IS-54", Wireless Personal Communications, 1, pp. 221-228, 1995.

[8] Gitlin, R. D., Hayes, J. F., and Weinstein, S. B., "Data Communications Principles", pp. 357-361, Plenum Press, 1992.

[9] Hashemi, H, "Simulation of the urban radio propagation channel", IEEE transactions on Vehicular Technology, VT-28, pp. 213-225, August 1979

[10] Hon, A. S., "An introduction to Paging - What it is and How it works?", Motorola Electronics Pte Ltd, 1993.

[11] Jakes, W. C., " Microwave Mobile Communications",pp. 235, IEEE press, 1994.

[12] Jordan, E. C., "Reference Data for Engineers: Radio, Electronics, Computer, and Communications", pp. 24-8, H. W. Sams & Co, 1986.

[13] Lee, E. A., and Messerschmitt, D. G.,"Digital Communications", pp. 206-209, Kluwer Acadamic Publishers, 1988.

[14] Lee, W. C. Y.,"Mobile Communications Engineering",pp. 402-403, McGraw-HIl Book Company, 1982.

[15] Macario, R. C. V., "Personal & Mobile Radio Systems", Peter Peregrinus Ltd on behalf of the Institution of Electrical Engineers, 1991.

[16] Mitra, S. K., and Kaiser, J. F., "Handbook for Digital Signal Processing", John Wiley & Sons Inc, 1993.

[17] Motorola Communications Device Data, "VHF Narrowband FM Receiver Design Using the MC 3362 and MC 3363 Dual Conversion Receivers", pp. (4-222) - (4-235).

[18] Oppenheim, A. V., and Schafer, R. W., "Discrete-Time Signal Processing", Prentice-Hall, !989.

[19] Sandvos, J. L., "A Comparison of Binary Paging Codes", IEEE Vehicular Technology Conference, May 1982.

[20] Schumacher, P. M., "Understand the basics of Spread - Spectrum communications", Microwave & RF, May 1993.

[21] Sklar, B., "Digital Communications, Fundamentals and Applications", pp. 150-154, Prentice Hall, 1988.

[22] Viterbi, A. J., " Spread Spectrum Communications - Myths and Realities", IEEE Communications Magazine, May 1979.

[23] Voelcker, H., "Toward a unified theory of modulation-part 1: phase-envelope relationships", Proceedings of the IEEE, vol. 54, pp. 340-353, March 1966.